



**Evaluation of Anthropogenic Emissions and Ozone Pollution in the North China Plain:  
Insights from the Air Chemistry Research in Asia (ARIAs) Campaign**

Hao He<sup>1</sup>, Xinrong Ren<sup>1,2,3</sup>, Sarah E. Benish<sup>1</sup>, Zhanqing Li<sup>1,4,5</sup>, Fei Wang<sup>5,6</sup>, Yuying Wang<sup>5</sup>,  
Timothy P. Canty<sup>1</sup>, Xiaobo Dong<sup>7</sup>, Feng Lv<sup>7</sup>, Yongtao Hu<sup>8</sup>, Tong Zhu<sup>9</sup>, and Russell R.  
Dickerson,<sup>1,4</sup>

<sup>1</sup>Department of Atmospheric and Oceanic Science, University of Maryland, College Park, MD  
20742, USA

<sup>2</sup>Air Resources Laboratory, National Oceanic and Atmospheric Administration, College Park,  
MD 20742, USA

<sup>3</sup>Cooperative Institute for Climate and Satellites, University of Maryland, College Park,  
Maryland, USA

<sup>4</sup>Earth System Science Interdisciplinary Center, University of Maryland, College Park, MD  
20740, USA

<sup>5</sup>College of Global Change and Earth System Science, Beijing Normal University, Beijing,  
100875, China

<sup>6</sup>Key Laboratory for Cloud Physics, Chinese Academy of Meteorological Sciences, Beijing,  
100081, China

<sup>7</sup>Weather Modification Office of Hebei Province, Shijiazhuang, 050021, China

<sup>8</sup>School of Civil & Environmental Engineering, Georgia Institute of Technology, Atlanta, GA  
30332, USA

<sup>9</sup>College of Environmental Sciences and Engineering, Peking University, Beijing 100871, China

**Keywords:** Ozone Production Sensitivity, Airborne Measurements, OMI, CMAQ

Corresponding to Dr. Hao He ([haohe@umd.edu](mailto:haohe@umd.edu))



### Abstract

To study the air pollution in the North China Plain (NCP), the Air Chemistry Research in Asia (ARIAs) campaign conducted airborne measurements of air pollutants including O<sub>3</sub>, CO, NO and NO<sub>2</sub> in spring 2016. High concentrations of pollutants, >100 ppbv of O<sub>3</sub>, >500 ppbv of CO, and >10 ppbv of NO<sub>2</sub>, were observed throughout the boundary layer during the campaign. CMAQ simulations with the 2010 EDGAR emissions can capture the basic spatial and temporal variations of ozone and its major precursors such as CO, NO<sub>x</sub> and VOCs, but significantly underestimate their concentrations. Observed emission enhancements of CO and NO<sub>x</sub> with respect to CO<sub>2</sub> suggest the existence of combustion with high emissions such as biomass burning in the NCP. The comparison with emission factors from the 2010 EDGAR emission inventory indicates that the contribution of combustion with high emissions has been overestimated. Differences between CMAQ simulations with 2010 emissions and satellite observations in 2016 can reflect the change in anthropogenic emissions. NO<sub>x</sub> emissions decreased in megacities such as Beijing and Shanghai confirming the effectiveness of recent control measures in China, while in other cities and rural areas NO<sub>x</sub> emissions slightly increased, e.g., CMAQ predicts only ~80% of NO<sub>x</sub> observed in the aircraft campaign area. CMAQ also underestimates HCHO (a proxy of VOCs, by ~20%) and CO (by ~60%) over the NCP, suggesting adjustments of the 2010 EDGAR emissions are needed to improve the model performance. HCHO/NO<sub>2</sub> column ratios derived from OMI measurements and CMAQ simulations show that VOC-sensitive chemistry dominates the ozone photochemical production in eastern China, suggesting the importance of tightening regulations on VOCs emissions. We adjusted EDGAR emissions based on satellite observations, conducted sensitivity experiments of CMAQ, and achieved better model performance in simulating ozone, but underestimation still exists. Because of the VOC-sensitive environment in ozone chemistry over the NCP, future study and regulations should focus on VOCs emissions with the continuous controls on NO<sub>x</sub> emissions in China.



## 56 1. Introduction

57 With rapid economic growth in the past three decades, the consumption of energy in  
58 China increased dramatically (Zhang and Cheng, 2009; Guan et al., 2018; Shan et al., 2018).  
59 Fossil fuels dominate total energy consumption, with coal still accounting for more than 50% of  
60 the carbon dioxide (CO<sub>2</sub>) emissions in China (Shan et al., 2018). This drastic increase in fossil  
61 fuel energy consumption is accompanied with deterioration of air quality (Chan and Yao, 2008;  
62 Fang et al., 2009), posing a threat to public health (Tie et al., 2009; Kan et al., 2012; Chen et al.,  
63 2013; Lelieveld et al., 2015). Particulate matter (PM) pollution, especially PM<sub>2.5</sub> in the North  
64 China Plain (NCP), drew public concern and governmental actions (He et al., 2001; Ye et al.,  
65 2003; Wang et al., 2005; Sun et al., 2006; Yang et al., 2011; Zhang et al., 2012; Zhang et al.,  
66 2013). PM pollution also has complex interactions with the planetary boundary layer (PBL) and  
67 its evolution, which can further degrade the air quality (Guo et al., 2016; Li et al., 2017b). Recent  
68 studies showed that tropospheric ozone (O<sub>3</sub>) pollution increased in China which exacerbated its  
69 complex air pollution problem (Xue et al., 2014; Verstraeten et al., 2015; Wang et al., 2017b; Ni  
70 et al., 2018).

71 Elevated ozone concentrations have adverse impacts on both human health (WHO, 2003;  
72 Anderson, 2009; Jerrett et al., 2009) and the ecosystem (Adams et al., 1989; Chameides et al.,  
73 1999; Ashmore, 2005). Tropospheric ozone absorbs thermal radiation and acts as the third most  
74 important anthropogenic contribution to radiative forcing of climate (Ramanathan and  
75 Dickinson, 1979; Lacis et al., 1990; IPCC, 2014). In the lower troposphere, the photolysis of  
76 ozone is an important source of atmospheric hydroxyl (OH) radicals that control the lifetimes of  
77 atmospheric species such as CO and volatile organic compounds (VOCs) (Logan et al., 1981;  
78 Thompson, 1992; Finlayson-Pitts and Pitts, 1999). Tropospheric ozone has a relatively long  
79 lifetime of several days to weeks (Stevenson et al., 2006; Young et al., 2013), leading to  
80 significant long-range transport of ozone and its precursors (Jacob et al., 1999; Derwent et al.,  
81 2004; Lin et al., 2008). Thus, investigation of ozone pollution in China is essential to support the  
82 national and international policy decision for air quality and the climate.

83 Tropospheric ozone is produced through complex photochemical reactions of precursors  
84 including nitrogen oxides (NO<sub>x</sub> = NO + NO<sub>2</sub>) and VOCs in the presence of sunlight  
85 (Haagensmit, 1952; Crutzen, 1974; Fishman et al., 1979; Seinfeld and Pandis, 2006). In China,  
86 sectors of power generation, industry, and transportation dominates the NO<sub>x</sub> emissions (Streets et



87 al., 2003; Ohara et al., 2007; Zhao et al., 2013a). Before 2010, NO<sub>x</sub> emissions in China increased  
88 substantially (Lin et al., 2010a; Zhao et al., 2013c). Analysis of satellite data revealed that  
89 recently NO<sub>x</sub> emissions have started decreasing in highly developed regions such as the Pearl  
90 River Delta (PRD), but still increased in other regions (Gu et al., 2013; Duncan et al., 2016; Liu  
91 et al., 2016). Anthropogenic VOCs emissions had a similar increasing trend in the past decades  
92 (Bo et al., 2008; Wei et al., 2011; Kurokawa et al., 2013; Zhao et al., 2017) and are projected to  
93 increase in the future (Zhang et al., 2018). Therefore the recent increase of tropospheric ozone in  
94 China could likely be explained by the enhanced anthropogenic emissions of ozone precursors.

95 Due to the complex O<sub>3</sub>-NO<sub>x</sub>-VOCs chemistry, we need to investigate the photochemical  
96 regime for local ozone production, i.e., NO<sub>x</sub>-sensitive or VOC-sensitive (Dodge, 1987;  
97 Kleinman, 1994). Duncan et al. (2010) used the ratio of tropospheric columns of formaldehyde  
98 (HCHO) and nitrogen dioxide (NO<sub>2</sub>) observed by the National Aeronautics and Space  
99 Administration (NASA) Aura Ozone Monitoring Instrument (OMI) to characterize ozone  
100 sensitivity. Studies show that a NO<sub>x</sub>-sensitive regime dominates in the United States, except in  
101 megacities such as Los Angeles and New York City where the local ozone production is in VOC-  
102 sensitive or in transition regimes (Duncan et al., 2010; Jin et al., 2017; Ring et al., 2018).  
103 However, VOC-sensitive and transition regimes for ozone photochemical production exist  
104 ubiquitously in China due to large amount of NO<sub>x</sub> emissions, especially over the NCP (Chou et  
105 al., 2009; Xing et al., 2011; Jin and Holloway, 2015; Jin et al., 2017). As such, although the  
106 current regulations in China focus only on reduction of NO<sub>x</sub> emissions (Wang and Hao, 2012;  
107 Wang et al., 2014a), air quality might also benefit from VOCs controls.

108 Aircraft measurements are essential to study the precursor emissions, photochemical  
109 production, and transport of ozone pollution at regional scale. However, airborne campaigns are  
110 sparse in China (Dickerson et al., 2007; Zhang et al., 2014; Ding et al., 2015; Huang et al., 2015;  
111 Wang et al., 2017a). To better understand the characteristics of ozone pollution, the Air  
112 Chemistry Research in Asia (ARIAs) aircraft campaign was conducted in Hebei Province of the  
113 NCP during May-June 2016, which was affiliated with the surface Aerosol Atmosphere  
114 Boundary-Layer Cloud (A<sup>2</sup>BC) experiment (Wang et al., 2018a; Wang et al., 2018b).  
115 Concentrations of major air pollutants in the lower atmosphere were measured during 11  
116 research flights in the NCP, which were conducted in association with the NASA Korea U.S. –  
117 Air Quality (KORUS-AQ) campaign in downwind South Korea. Measurements collected in the



ARIAs research flights and the A<sup>2</sup>BC surface observations provide a comprehensive dataset to thoroughly study the tropospheric ozone pollution and emissions of its precursors in China.

In this study, we evaluate anthropogenic emissions and the ozone pollution in the NCP using a combination of aircraft measurements, surface monitoring data, satellite observations, and modeling results. The Environmental Protection Agency (EPA) Community Multiscale Air Quality (CMAQ) model was used to simulate the atmospheric chemistry for the ARIAs campaign. We evaluate the emission data by comparing with the aircraft measurements and satellite products, and then adjust emissions to improve the CMAQ performance. Lastly, we investigate the sensitivity of ozone production derived from CMAQ simulations and OMI observations and discuss the future ozone pollution in China.

## 2. Data and Method

### 2.1 Aircraft campaign in the NCP

With more than 250 million tons of iron and steel produced in 2016 (data from <http://data.stats.gov.cn>, accessed in September 2018), Hebei Province in the NCP is the most industrialized area in China. Due to its high emissions and proximity to megacities Beijing and Tianjin, the Beijing-Tianjin-Hebei area has experienced severe air pollution in the past decade (Zhao et al., 2013b; Wang et al., 2014b). In May and June 2016, the ARIAs aircraft campaign was conducted over Hebei Province to investigate the emissions, chemical evolution, and transport of air pollutants. The airborne campaign was coordinated with the A<sup>2</sup>BC field campaign in Xingtai (XT, 37.18 °N, 114.36 °E, 182 m above sea level, ASL) and the NASA KORUS-AQ campaign to expand the study to East Asia. A Harbin Y12 research airplane (similar to the de Havilland Twin Otter) was employed to measure concentrations of air pollutants including O<sub>3</sub>, carbon monoxide (CO), CO<sub>2</sub>, NO<sub>2</sub>, and aerosol optical properties. The research airplane was located in Luancheng airport, hereafter referred to as LC (LC, 37.91 °N, 114.59 °E, 58 m ASL), south of Shijiazhuang, the capital city of Hebei province with a population of 10 million. Eleven research flights were conducted during the ARIAs campaign (Fig. 1a). Vertical profiles of air pollutants from near surface (~100 m above ground level, AGL) to the free troposphere (> 3000 m) were conducted over LC, XT (the supersite of the A<sup>2</sup>BC campaign), Julu (JL, 37.22 °N, 115.02 °E, 30 m ASL), and Quzhou (QZ, 36.76 °N, 114.96 °E, 40 m ASL).

The airborne measurements of ozone were conducted using a commercially available



analyzer (Model 49C, Thermo Environmental Instruments, TEI, Franklin, Massachusetts) (Taubman et al., 2006). NO<sub>2</sub> was measured using a modified commercially available cavity ring-down spectroscopy (CRDS) detector (Castellanos et al., 2009; Brent et al., 2013). Concentrations of CO and CO<sub>2</sub> were monitored with a 4-channel Picarro CRDS instrument (Model G2401-m, Picarro Inc., Santa Clara, CA), calibrated with CO/CO<sub>2</sub> standards certified at the National Institute of Standards and Technology (Ren et al., 2018). All the instruments were routinely serviced, calibrated and used for airborne measurements in the United States and China (Taubman et al., 2006; Dickerson et al., 2007; Hains et al., 2008; He et al., 2012; He et al., 2014; Ren et al., 2018; Salmon et al., 2018). Measurements of ambient air pollutants were made at 1 Hz frequency and synchronized with time, geolocation and altitude from the Global Position System (GPS).

In the ARIAs research flights, 28 whole air samples (WAS) were collected in vertical spirals at different altitudes from ~400 m to ~3500 m. The WAS were analyzed using gas chromatography (GC) with Flame Ionization Detection (FID) and Mass Spectroscopy (MS) by the College of Environmental Sciences and Engineering at Peking University. 74 species of alkanes, alkenes/alkynes, aromatics, and halocarbons were identified and quantified for a study on ozone photochemical chemistry (see details in Benish et al., 2019). Detection limits for the compounds ranged from 2 to 50 pptv. Surface observation of trace gases including O<sub>3</sub>, CO, NO, and NO<sub>x</sub> were measured at the A<sup>2</sup>BC Xingtai supersite using analyzers manufactured by Ecotech (Wang et al., 2018b); detailed description of the analyzers is discussed in Zhu et al. (2016). Surface HCHO concentrations were monitored using a formaldehyde analyzer (AERO LASER, Germany, Model 4021) based on fluorometric Hantzsch reactions (Gilpin et al., 1997; Rappenglück et al., 2010). All surface observations were collected as 1-min averaged data and processed to hourly mean values.

173

## 2.2 Satellite products

To evaluate the emissions and atmospheric chemistry in the NCP and greater East Asia, we used satellite observations of CO, NO<sub>2</sub>, and HCHO for May and June 2016. The Measurements of Pollution In the Troposphere (MOPITT) instrument onboard the NASA Terra satellite retrieved CO column contents with ~10:30 am local overpass time (Deeter et al., 2003). We used the latest version 7 MOPITT Level 3 daily gridded average products (1° × 1° spatial



180 resolution, available at [https://eosweb.larc.nasa.gov/project/mopitt/mop03j\\_v007](https://eosweb.larc.nasa.gov/project/mopitt/mop03j_v007)) for the ARIAs  
 181 campaign period (MOPITT Science Team, 2013). MOPITT thermal-infrared and near-infrared  
 182 (TIR + NIR) products shows improved sensitivity to near surface CO in China (Worden et al.,  
 183 2010). We used MOPITT near surface CO ( $\sim 900$  hPa) products and related averaging kernels  
 184 (AKs) to evaluate the CMAQ results (Deeter et al., 2012).

185 OMI, onboard the NASA Aura satellite, is a UV/Vis solar backscatter spectrometer in a  
 186 polar sun-synchronous orbit with a  $\sim 1:35$  pm local overpass time. With high spatial resolution  
 187 ( $13 \text{ km} \times 24 \text{ km}$  for the center at nadir) and nearly daily coverage, OMI has provided monitoring  
 188 of trace gases and aerosol properties since 2005 (Levelt et al., 2006). The Version 3 OMI Level 2  
 189  $\text{NO}_2$  products ([https://disc.gsfc.nasa.gov/datasets/OMNO2\\_V003/summary](https://disc.gsfc.nasa.gov/datasets/OMNO2_V003/summary)) (Krotkov et al.,  
 190 2018) were used to evaluate the emissions and atmospheric chemistry in East Asia. Under clear  
 191 sky, tropospheric  $\text{NO}_2$  columns from OMI has precision of  $\sim 0.5 \times 10^{16}$  molecules  $\text{cm}^{-2}$  and an  
 192 accuracy of  $\pm 30\%$  (Krotkov et al., 2017). OMI HCHO Version 3 Smithsonian Astronomical  
 193 Observatory (SAO) ([https://disc.gsfc.nasa.gov/datasets/OMHCHO\\_V003/summary](https://disc.gsfc.nasa.gov/datasets/OMHCHO_V003/summary)) Level 2  
 194 products were used in this study (Chance, 2007; González Abad et al., 2015). The precision of  
 195 column HCHO is  $\sim 1.0 \times 10^{16}$  molecules  $\text{cm}^{-2}$  and SAO products have an accuracy of  $\pm 25\text{--}30\%$   
 196 without cloud (Millet et al., 2006; Boeke et al., 2011). Data in OMI pixels affected by the row  
 197 anomaly and contaminated by clouds were filtered out using quality flags for both  $\text{NO}_2$  and  
 198 HCHO columns.

199

## 200 **2.3 Model set-up**

201 We used CMAQ version 5.2 (EPA, 2017) to simulate atmospheric chemistry for the  
 202 ARIAs campaign. The Weather Research and Forecasting (WRF) model Version 3.8.1  
 203 (Skamarock et al., 2008) was driven by the European Centre for Medium-Range Weather  
 204 Forecasts (ECMWF) ERA-Interim products (ds627.0, <https://rda.ucar.edu/datasets/ds627.0>) (Dee  
 205 et al., 2011) to simulate meteorological fields. Two domains with spatial resolution of 36 km and  
 206 12 km (Fig. 1b) were used to cover East Asia, with 35 layers from the surface to 50 hPa and  $\sim 20$   
 207 layers in the lowest 2 km. Major physical options in WRF include the Rapid Radiative Transfer  
 208 Model (RRTM) radiation scheme (Clough et al., 2005), the Pleim-Xiu surface layer and land  
 209 surface model (Pleim and Xiu, 1995; Xiu and Pleim, 2001), the Asymmetric Convective Model  
 210 (ACM2) boundary layer scheme (Pleim, 2007), the Kain-Fritsch cumulus scheme (Kain, 2004),





211 and the WRF Single-Moment 6 (WSM-6) microphysics (Hong and Lim, 2006). The National  
212 Centers for Environmental Prediction (NCEP) ADP Global Surface and Upper Air Observational  
213 Weather Data (ds461.0 and ds351.0, <https://rda.ucar.edu>) were used to perform observational and  
214 analysis nudging on all domains following the method developed for NASA aircraft campaigns  
215 (He et al., 2014; Mazzuca et al., 2016). WRF outputs were processed by the EPA Meteorology-  
216 Chemistry Interface Processor Version 4.3 (MCIP v4.3, released in November 2015) for emission  
217 processing and CMAQ simulations.

218 Anthropogenic emissions were from the Emissions Database for Global Atmospheric  
219 Research Version 4.2 (EDGAR v4.2,  $0.1^\circ \times 0.1^\circ$  resolution) of year 2010, which are widely used  
220 for chemical transport modeling (European Commission, 2011). We used the EPA Sparse Matrix  
221 Operator Kernel Emissions (SMOKE) modeling system Version 4.5 (UNC, 2017) to project  
222 EDGAR emissions to the modeling domain. Emissions of air pollutants were speciated into  
223 Carbon Bond 05 chemical mechanism (Yarwood et al., 2005) and updated AERO6 aerosol  
224 module (Appel et al., 2013). The EDGAR v4.2 inventory has emissions for energy, industry,  
225 residential, and transport sectors. Without stack height information for power plants in the energy  
226 sector, we followed the approach developed in He et al. (2012) to locate these anthropogenic  
227 emissions at  $\sim 200$  m above the surface as an approximation for averaged stack height and plume  
228 rise. We used the United States Geological Survey (USGS) 24 category land use dataset  
229 combined with the Biogenic Emission Inventory System (BEIS) emission factors table to  
230 generate the input files for the CMAQ inline biogenic emissions modeling. Biogenic emissions  
231 were estimated using the BEIS module inline in CMAQ (EPA, 2017).

232 CMAQ v5.2 uses the updated Carbon Bond 6 (CB6r3) chemical mechanism (Yarwood et  
233 al., 2010) including improved chemistry mechanism for organic nitrates and peroxyacyl nitrates  
234 (PAN) chemistry and will lead to better performance for simulating Secondary Organic Aerosols  
235 (SOA) and tropospheric ozone in the United States (Appel et al., 2016). CMAQ was run with a  
236 coarse domain and a nested domain (Fig. 1b). Chemical initial and boundary conditions for the  
237 coarse domain were obtained from the default concentration profiles built in CMAQ (EPA,  
238 2017). Results from the CMAQ coarse domain were used to generate boundary conditions for  
239 the nested domain. The WRF-CMAQ system was run from mid-April to June with the first 2  
240 weeks as spin-up. Hourly concentrations of air pollutants were saved for further analysis and  
241 model evaluation.





### 3. Results and discussion

#### 3.1 Air Pollution in the NCP and CMAQ performance

Figure 2 summarizes all aircraft measurements of O<sub>3</sub>, NO<sub>2</sub>, CO, and CO<sub>2</sub> over the NCP from eleven research flights. Generally, we observed high concentrations of trace gases, such as >100 part per billion by volume (ppbv) of O<sub>3</sub>, >20 ppbv of NO<sub>2</sub>, >500 ppbv of CO, and >450 part per million by volume (ppmv) of CO<sub>2</sub>, in the aircraft campaign area (defined as 36.5–38.5°N, 114.0–115.5°E hereafter). We conducted vertical spirals over XT (the A<sup>2</sup>BC supersite), LC (the airport in south of Shijiazhuang), and two rural areas (JL and QZ) during the ARIAs research flights. Figure 3a summarizes vertical distributions and the mean profiles of air pollutants over XT, with mean O<sub>3</sub> concentrations of 80 ppbv in the lower atmosphere. We observed isolated plumes with >10 ppbv of NO<sub>2</sub>, >1000 ppbv of CO, and >440 ppmv of CO<sub>2</sub> over XT, usually with a secondary maximum between 800 and 1200 m. These plumes aloft can play an important role in long-range transport of air pollutants to downwind regions. Profiles over LC (Fig. 3b) show higher O<sub>3</sub> concentrations (>100 ppbv) and relatively moderate NO<sub>2</sub> (~3 ppbv) and CO (~250 ppbv). The rural areas, JL and QZ, have relatively clean environment with <80 ppbv of O<sub>3</sub>, <2 ppbv of NO<sub>2</sub>, and <300 ppbv of CO (Fig. 3c and 3d). Even the concentrations of air pollutants over the rural region in the NCP are comparable or higher than values in urban areas in North America and Europe. In summary, we found the south-north and east-west gradients of air pollution, i.e., higher concentrations of air pollutants in the west XT-LC corridor near the mountain as compared with east side of JL and QZ. Thus, the ARIAs research flights have good coverage of regions with both high and moderate concentrations of air pollutants and can fairly represent the regional nature of air pollution over the NCP.

Comparison of the surface trace gas observations at the Xingtai supersite and the CMAQ simulations driven by the EDGAR inventory (named baseline CMAQ case hereafter) reveals that CMAQ generally underestimates concentrations of major air pollutants (Fig. S1 in the supplementary material). The baseline CMAQ run successfully captures the diurnal and daily variations of surface ozone in Xingtai, although consistently underpredicts its concentrations. For CO and NO<sub>x</sub>, two important ozone precursors, CMAQ substantially underestimates their concentrations in Xingtai by more than 50% and especially fails to capture the extremely high values such as 6–7 ppmv of CO and ~100 ppbv of NO<sub>x</sub>. This underestimation could be caused by local sources poorly represented in the 12-km model simulations. For ambient HCHO, an



important byproduct of VOC oxidization in ozone photochemical production, the baseline CMAQ run captures the variations, but substantially underestimates its concentrations. These results suggest that the underestimation of ozone precursors in CMAQ could lead to the poor model performance of simulating tropospheric ozone and other pollutants.

Similar analyses were conducted to investigate air pollutant concentrations in the lower troposphere over the NCP observed by the aircraft. A case of the research flight on June 11, 2016 (Fig. S2 in the supplementary material) shows that CMAQ well captures the vertical gradient of air pollutants, while substantially underestimates concentrations of all trace gases except  $\text{NO}_y$ . Following the approach described in Goldberg et al. (2016), we calculated the 10-min average  $\text{O}_3$ , CO, NO, and  $\text{NO}_2$  concentrations from aircraft measurements and compared them with the baseline CMAQ simulations (Fig. 4) and found similar underestimation (50% to 75% for all air pollutants) as compared with surface measurements (Fig. S1 in the supplementary material). CMAQ overestimates  $\text{NO}_y$  but substantially underestimates NO and  $\text{NO}_2$ , which suggests that a significant amount of reactive nitrogen compounds could exist in the format of organic nitrates or nitrate aerosols in the model. Figure 5 compares total VOCs concentrations from WAS samples and CMAQ simulations, indicating that VOCs levels are significantly underestimated by 80%. The model evaluation with surface and aircraft measurements suggest that in the NCP ozone pollution has been significantly underestimated in the baseline CMAQ run, which could be due to the uncertainty introduced by using the 2010 EDGAR emissions to simulate the 2016 ARIAs campaign period. Thus, we need to evaluate the emissions inventory data to improve the CMAQ performance and investigate the sensitivity of ozone production.

### 3.2 Evaluation of emissions inventory in the NCP

The EDGAR v4.2 emission inventory in East Asia was created based on the 2010 MIX emission inventory (Li et al., 2017a), so substantial changes were anticipated when used for the ARIAs campaign in 2016. Anthropogenic emission inventories are usually based on the “bottom-up” approach, which relies on the statistics of fossil fuel usage and emission factors (EFs) for each sector defined as the ratio of the amount of air pollutants released by a unit of  $\text{CO}_2$  emissions, e.g.  $\text{CO}/\text{CO}_2$  and  $\text{NO}_x/\text{CO}_2$ . To evaluate the emission inventory data in the NCP, we used a 60-s moving window and conducted linear regression of observed air pollutant (CO,  $\text{NO}_x$ , etc.) concentrations vs.  $\text{CO}_2$  concentrations, i.e.  $\Delta\text{CO}/\Delta\text{CO}_2$  and  $\Delta\text{NO}_x/\Delta\text{CO}_2$ , defined as



304 emission enhancements (EEs). Through only selecting EEs that are in the PBL (below 1.5 km  
305 AGL in this study) and statistically significant ( $R^2 > 0.6$ ), the values of EEs can act as a proxy of  
306 EFs in the air mass observed (Halliday et al., 2018).

307 EEs observed during the research flights have a broad range of values.  $\Delta\text{CO}/\Delta\text{CO}_2$  ranges  
308 from below 1%, a typical value of modern automobile emissions, to higher than 10%, a value  
309 indicating fossil fuel combustion with high emissions such as biomass burning (Fig. 6a and 6b).  
310 The mean of observed EE for CO (3.7%) is close to that calculated from the EDGAR inventory  
311 (4.0%) in the aircraft campaign area. Observed  $\Delta\text{NO}_x/\Delta\text{CO}_2$  ratios also have isolated high values  
312 ( $>0.1\%$ ) with a mean value of 0.05%, which is substantially higher than the EF ( $\sim 0.03\%$ ) derived  
313 from the EDGAR inventory. Since estimation of anthropogenic  $\text{CO}_2$  flux in an urban/suburban  
314 area is challenging (Cambaliza et al., 2014; Heimbürger et al., 2017), the underestimation of CO  
315 and  $\text{NO}_x$  in the NCP could be caused by either underestimated EFs or uncertainty in  
316 anthropogenic  $\text{CO}_2$  emission data used in the ‘bottom-up’ approach.

317 To further investigate the characteristics of air pollutant emissions in the NCP, we  
318 conducted a similar analysis of  $\Delta\text{NO}_x/\Delta\text{CO}$ , which are usually co-emitted in combustion  
319 processes. Since around half of the CO and  $\text{NO}_x$  are from mobile sources in the EDGAR  
320 emission inventory, this ratio can approximately represent the emission characteristic of mobile  
321 sources in the NCP. The mean observed  $\Delta\text{NO}_x/\Delta\text{CO}$  ratio is  $\sim 1.3\%$ , significantly lower than  
322 5.6% based on the EDGAR emission inventory (Fig. 6c). These results suggest that the EDGAR  
323 emission inventory substantially overestimates the ratios of  $\text{NO}_x/\text{CO}$ , while the automobile  
324 emissions over the NCP in 2016 have been greatly improved due to recent regulations focusing  
325 on  $\text{NO}_x$ , i.e., EDGAR overestimates the contribution from combustion with high emissions. It is  
326 worth noting that we only evaluated the emission ratios (EEs or EFs) in the EDGAR inventory,  
327 while the underestimation of CO and  $\text{NO}_x$  emissions could be caused by inaccurate  $\text{CO}_2$   
328 emissions which have not been examined in this study.

329

### 330 **3.3 Evaluation of CO, $\text{NO}_x$ , and VOCs emissions using satellite data**

331 Satellite observations are widely used to evaluate the anthropogenic emissions in East  
332 Asia sometimes supplemented by model simulations, e.g., CO emissions using the MOPITT CO  
333 products (Jiang et al., 2015; Zheng et al., 2018), anthropogenic  $\text{NO}_x$  emissions using OMI  $\text{NO}_2$   
334 products (Wang et al., 2012; de Foy et al., 2015; Qu et al., 2017), and VOCs emissions using



335 OMI HCHO products (Stavrakou et al., 2016). In this study, we used measurements from  
336 multiple satellite instruments to evaluate the CMAQ performance of NO<sub>2</sub>, HCHO, and CO. Since  
337 NO<sub>2</sub> and HCHO can be treated as proxy of NO<sub>x</sub> and VOCs emissions, we can further improve  
338 the 2010 EDGAR emissions over the NCP base on satellite data.

339 We followed the approach developed in Canty et al. (2015) to compare the tropospheric  
340 column contents of NO<sub>2</sub> from OMI products and CMAQ simulations. Level 2 OMI NO<sub>2</sub> swath  
341 information including row anomaly and quality flags were used to sample NO<sub>2</sub> vertical profiles  
342 from CMAQ outputs, and then CMAQ NO<sub>2</sub> column was calculated using the OMI averaging  
343 kernel (AK). Lastly, we averaged OMI and CMAQ NO<sub>2</sub> column contents to create daily 0.25° ×  
344 0.25° Level 3 products (see details in Canty et al., 2015). A similar approach was used to  
345 integrate HCHO column contents from CMAQ simulations based on OMI HCHO retrievals (see  
346 details in Ring et al., 2018) and construct daily 0.25° × 0.25° Level 3 HCHO products. For  
347 tropospheric CO, we selected the CO concentrations at ~ 900 hPa in CMAQ and averaged them  
348 to 1.0° × 1.0° daily products using MOPITT CO averaging kernel (MOPITT Science Team,  
349 2013). All gridded daily data of satellite and CMAQ were averaged in May and June 2016 for  
350 comparison.

351 Figure 7a shows strong signals over the NCP of the OMI NO<sub>2</sub> observations. CMAQ  
352 underestimates NO<sub>2</sub> columns over the aircraft campaign area, and only predicts 81% of NO<sub>2</sub>  
353 column as compared with OMI observations. However, in urban regions such as Beijing, the  
354 Yangtze River Delta (YRD), and the PRD, CMAQ substantially overestimates column NO<sub>2</sub> by  
355 up to 30%. Because the baseline CMAQ simulations used the 2010 anthropogenic emission data,  
356 these differences should reflect the changes in NO<sub>x</sub> emissions due to recent air pollution  
357 regulations. The comparison of NO<sub>2</sub> column suggests that NO<sub>x</sub> pollution of megacities in China  
358 has been substantially improved after 2010 while NO<sub>x</sub> pollution in smaller cities and rural area  
359 has worsened, consistent with results from independent studies using OMI (Duncan et al., 2016;  
360 Krotkov et al., 2016). OMI HCHO retrievals also show high values over the NCP in spring when  
361 plants' photosynthetic activity is relatively low, reflecting that the domination of anthropogenic  
362 VOCs emissions in north China (Zhao et al., 2017). CMAQ has good agreement with OMI  
363 HCHO within the aircraft campaign area (<20% underestimation), but substantially  
364 underestimates HCHO columns in south China where biogenic VOCs dominate (Fig. 7b). The  
365 MOPITT products show high near-surface CO concentrations over the eastern China (Fig. 7c),



while the baseline CMAQ run substantially underestimates CO concentrations over north China and only predicts 42% of the CO over the aircraft campaign area.

Using NO<sub>2</sub> and HCHO as proxies of NO<sub>x</sub> and anthropogenic VOCs emissions, the comparison of satellite observations and the baseline CMAQ simulations suggests that both NO<sub>x</sub> and VOCs emissions in the aircraft campaign area need to be adjusted for a better simulation of tropospheric ozone. Also, the underestimation of CO, as an important precursor, can lead to underprediction of tropospheric ozone. We calculated the model/satellite ratios of NO<sub>x</sub>, HCHO, and CO in East Asia (Fig. 8) and used these ratios to adjust their anthropogenic emissions in CMAQ. The results will be discussed in Section 3.4.

### 3.3 Tropospheric ozone production sensitivity from OMI and CMAQ

Photochemical production of tropospheric ozone is highly non-linear and dependent on concentrations of NO<sub>x</sub> and VOCs (Kleinman, 1994; Sillman, 1999; Kleinman, 2000). A maximum rate of ozone production can be achieved with an optimal VOCs/NO<sub>x</sub> ratio. With other VOCs/NO<sub>x</sub> ratios, ozone production can be either in the VOC-sensitive regime (the rate of ozone production is controlled by VOCs concentrations) or in the NO<sub>x</sub>-sensitive regime (the rate of production is controlled by NO<sub>x</sub> concentrations). Different pollution control strategies can be implemented to reduce the tropospheric ozone levels in these two regimes. For instance, in a VOC-sensitive environment, reducing NO<sub>x</sub> emissions will lead to limited effects until the ozone production has been changed to a NO<sub>x</sub>-sensitive environment with the continuous removal of NO<sub>x</sub> from the atmosphere. Duncan et al. (2010) developed an approach using OMI HCHO/NO<sub>2</sub> column ratio to estimate the ozone production sensitivity as: 1) HCHO/NO<sub>2</sub> < 1: VOC-sensitive regime; 2) HCHO/NO<sub>2</sub> 1~2: transition regime; 3) HCHO/NO<sub>2</sub> > 2: NO<sub>x</sub>-sensitive regime. Studies show that urban areas in the U.S. such as Los Angeles, New York City and Houston are in VOC-sensitive or transition regimes, which lead to difficulty in local regulation of air quality (Duncan et al., 2010; Mazzuca et al., 2016; Ring et al., 2018). Recent studies suggest new threshold values of HCHO/NO<sub>2</sub> ratios between VOC-sensitive, transition, and NO<sub>x</sub>-sensitive regimes in the U.S. (Jin et al., 2017; Schroeder et al., 2017).

Using the Duncan et al. (2010) approach, studies using OMI products suggest large areas of eastern China are either in VOC-sensitive regime (mostly megacities such as Beijing) or in transition regime (Jin and Holloway, 2015; Jin et al., 2017; Xing et al., 2018). We follow the



approach described in Ring et al. (2018) to calculate the column HCHO/NO<sub>2</sub> ratios from OMI observations and CMAQ simulations for East Asia. OMI column HCHO/NO<sub>2</sub> ratios suggest that the ozone photochemical production is VOC-sensitive or in transition region over the NCP and other major urban areas such as YRD and PRD (Fig. 9a) if the Duncan et al. (2010) approach is applicable for these areas. CMAQ successfully captured the spatial distribution of the regional nature of ozone production sensitivity in eastern China but predicted that the rate of ozone production is controlled more by VOCs with the CMAQ HCHO/NO<sub>2</sub> ratio lower than 1.0 in Beijing, YRD, and PRD (Fig. 9b). The VOC-sensitive environment suggests the rate of ozone photochemical production in the NCP is controlled not only by NO<sub>x</sub> emissions, but also by VOCs emissions which currently lack regulations in China. With continuous reduction of anthropogenic NO<sub>x</sub> emissions in China, VOCs controls might be efficient in these VOC-sensitive regions.

409

### 3.4 Improvements of tropospheric ozone simulation using satellite products

Results of the previous two sections show that the baseline CMAQ run substantially underestimates the concentrations of ozone and its major precursors in the NCP. To identify the individual and combined effects of the emission discrepancy of impacting major ozone precursors in the NCP, we designed a series of sensitivity experiments with emissions adjusted to satellite observations. Unlike the top-down approach using global chemical transport models such as GEOS-Chem (Lin et al., 2010b; Qu et al., 2017), here we simply applied the ratios of air pollutant column contents from satellite observations and CMAQ simulations on each 0.25 degree grids (Fig. 8) as: CO<sub>CMAQ</sub>/CO<sub>MOPIIT</sub>, NO<sub>2CMAQ</sub>/NO<sub>2OMI</sub>, and HCHO<sub>CMAQ</sub>/HCHO<sub>OMI</sub> ratios for anthropogenic CO, NO<sub>x</sub>, and VOCs emissions, respectively. To estimate the contribution from biogenic VOCs emissions, we conducted one more run with the in-line BEIS module turned off. Table 1 shows the emission adjustments for the five sensitivity experiments. CMAQ was run for the nested 12 km domain (D02) with the same meteorology, initial conditions, and boundary conditions derived from the coarse domain simulations.

Figure 10 presents the evaluation of surface observations with respect to two sensitivity experiments (CMAQ<sub>baseline</sub> and CMAQ<sub>all</sub>, comparison with all CMAQ runs are presented in Fig. S3 in the supplementary material). CMAQ still might not capture the extreme high values of surface O<sub>3</sub> and CO (Fig. 10a and 10b). For instance, the maximum CO concentration from





CMAQ simulations are ~1700 ppbv while surface observations have CO peaks higher than 6000 ppbv (Fig. 10b). The adjustments of the emission inventory have improved the model simulations of NO<sub>2</sub>/NO (Fig. 10c and 10d) and HCHO (Fig. 10e). During the ARIAs flights, we observed various sources of emissions in the aircraft campaign area such as small factories and biomass burning, which are not included in the EDGAR emission inventory. Thus, the reason for the model underestimation could be that the spatial resolution (12 km) of the nested CMAQ domain cannot represent the detailed emissions and resolve the local air pollution hotspots. However it is worth noting that even our CMAQ system is still not capable to reproduce the surface air quality at Xingtai, the adjustments of EDGAR emissions based on satellite observations reduce the underestimation.

The ARIAs flights covered a large area (~10<sup>4</sup> km<sup>2</sup>) in Hebei Province, which represent the regional nature of air pollution over the NCP. A case comparison of CMAQ\_All case and Y12 measurements on June 11, 2016 (Fig. 11) shows better results in both concentrations and vertical gradient of air pollutants (compared with Fig. S2 in the supplementary material), indicating the effectiveness of improving the emission inventories based on satellite observations. Table 2 summarizes the model performance of CMAQ as compared with aircraft measurements. The adjustments of the EDGAR emissions with satellite observations moderately improved simulations of ozone pollution, with the root mean square error (RSME) decreasing from 25.1 ppbv (the baseline case) to 21.2 ppbv (CMAQ\_All case) and the mean ratio of CMAQ simulations to aircraft observations increasing from 0.75 to 0.82. The model performance of CO has also been improved, with the RMSE decreasing from 247.0 ppbv to 203.6 ppbv and the mean ratio increasing from 0.40 to 0.66. For nitrogen compounds including NO<sub>2</sub>, NO, and NO<sub>y</sub>, the adjustments of EDGAR emissions have small impacts on improving the CMAQ performance. The reason could be that the ozone photochemistry is mainly VOC-sensitive over the NCP, so the adjustments of NO<sub>x</sub> emissions have limited impacts close to sources.

#### 4. Conclusions and Discussion

The ARIAs campaign conducted aircraft measurements over the NCP and observed high concentrations of air pollutants including O<sub>3</sub>, CO, and NO<sub>x</sub>. CMAQ simulations driven by the 2010 EDGAR emissions substantially underestimate the levels of ozone and its precursors in the campaign region. Analysis of emission enhancements of CO and NO<sub>x</sub> with respect to concurrent





CO<sub>2</sub> measurements suggests that the usage of the 2010 EDGAR emissions for the 2016 ARIAs campaign could introduce substantial uncertainty due to the recent changes of anthropogenic emissions in China. Comparison of atmospheric columns of NO<sub>2</sub> from CMAQ simulations and satellite observations suggests that NO<sub>x</sub> emissions decreased in megacities such as Beijing and Shanghai but increased in rural areas from 2010 to 2016. Similar analysis of HCHO and CO shows that the EDGAR VOCs and CO emissions could also be underestimated in the NCP. HCHO/NO<sub>2</sub> column ratio from OMI observations indicates tropospheric ozone production is mainly in the VOC-sensitive regime in the NCP, which is also confirmed by CMAQ simulations. To test a hypothesis that the poor model performance is due to emission biases, we adjusted the EDGAR emissions over East Asia based on satellite observations. Better performance of simulating ozone and its precursors is achieved, while underestimation still exists.

Both satellite observations and CMAQ simulations indicate that the VOC-sensitive chemistry dominates the ozone photochemical production in eastern China, so the rate of local ozone production is mainly controlled by the VOCs emissions. In the past few years, despite implementation of control measures mainly on SO<sub>2</sub> and NO<sub>x</sub>, ozone concentrations have increased in China. Our study indicated that high NO<sub>x</sub> concentrations were pervasive in the PBL over rural areas of the NCP, where anthropogenic VOCs were also abundant. Reducing NO<sub>x</sub> emissions is essential to control ozone on the regional scale, but our model simulations indicated that reducing VOCs emissions can lower the rate of photochemical smog production.

Currently, studies and regulations on anthropogenic VOCs emissions in China are lacking, so with expectation of further decreasing NO<sub>x</sub> emissions in China, more severe ozone pollution could be anticipated. It is worth noting that while VOCs controls can have beneficial impact on the local rate of ozone production in the VOC-sensitive regime, the ozone levels will not decrease until NO<sub>x</sub> emissions are substantially lower, i.e., regulations on VOCs are needed as well as the continuous controls on NO<sub>x</sub> emissions in China. These results can also partially explain why ozone pollution emerged in the past few years while PM<sub>2.5</sub> pollution has been substantially improved with strict regulations on anthropogenic emissions. New datasets such as the updated ‘bottom-up’ emissions inventory for East Asia and high resolution satellite observations such as TROPOMI and GEMS products are needed to improve the modeling of ozone pollution in China, which can provide scientific evidence for future national and international regulations on air quality.



490

491 **Author contribution**

492 X.R., R.D., H.H. and Z.L. designed the aircraft campaign; H.H., X.R., F.W., X.D., and F.L.  
493 performed the research flights; Y.W., X.R., and T.Z. conducted the surface observations; H.H.,  
494 T.P., and Y.H. developed the modeling system; H.H., X.R., and S.B. analyzed the data; H.H.,  
495 X.R., S.B. and R.D wrote the paper

496

497 **Acknowledgements**

498 This work was funded by the National Science Foundation of the United States (Grant 1558259).  
499 We thank all of the A<sup>2</sup>BC and ARIAs research team, especially the flight crew of Hebei Weather  
500 Modification Office's Y12 airplane. The flight campaign was conducted in association with the  
501 NASA's KORUS-AQ campaign.

502

503 **Disclaimer**

504 The scientific results and conclusions, as well as any views or opinions expressed herein, are  
505 those of the author(s) and do not necessarily reflect the views of NOAA or the Department of  
506 Commerce.

507

508 **References**

- 509 Adams, R. M., Glycer, J. D., Johnson, S. L., and McCarl, B. A.: A reassessment of the economic-effects of ozone on  
510 United-States agriculture, *Japca-the Journal of the Air & Waste Management Association*, 39, 960-968,  
511 1989.
- 512 Anderson, H. R.: Air pollution and mortality: A history, *Atmospheric Environment*, 43, 142-152,  
513 10.1016/j.atmosenv.2008.09.026, 2009.
- 514 Appel, K. W., Pouliot, G. A., Simon, H., Sarwar, G., Pye, H. O. T., Napelenok, S. L., Akhtar, F., and Roselle, S. J.:  
515 Evaluation of dust and trace metal estimates from the Community Multiscale Air Quality (CMAQ) model  
516 version 5.0, *Geoscientific Model Development*, 6, 883-899, 10.5194/gmd-6-883-2013, 2013.
- 517 Appel, K. W., Napelenok, S. L., Hogrefe, C., Foley, K. M., Pouliot, G., Murphy, B. N., Luecken, D. J., and Heath,  
518 N.: Evaluation of the Community Multiscale Air Quality (CMAQ) Model Version 5.2, 2016 CMAS  
519 Conference, Chapel Hill, NC., 2016.
- 520 Ashmore, M. R.: Assessing the future global impacts of ozone on vegetation, *Plant Cell Environ.*, 28, 949-964,  
521 10.1111/j.1365-3040.2005.01341.x, 2005.
- 522 Benish, S. E., He, H., Ren, X., Roberts, S., Li, Z., Wang, F., Zhang, F., Wang, Y., Shao, M., Lu, S., Pfister, G.,  
523 Flocke, F., and Dickerson, R.: Observations of Nitrogen Oxides and Volatile Organic Compounds over the  
524 North China Plain and Impact on Ozone Formation, In preparation, 2019.
- 525 Bo, Y., Cai, H., and Xie, S. D.: Spatial and temporal variation of historical anthropogenic NMVOCs emission  
526 inventories in China, *Atmospheric Chemistry and Physics*, 8, 7297-7316, 10.5194/acp-8-7297-2008, 2008.
- 527 Boeke, N. L., Marshall, J. D., Alvarez, S., Chance, K. V., Fried, A., Kurosu, T. P., Rappenglück, B., Richter, D.,  
528 Walega, J., Weibring, P., and Millet, D. B.: Formaldehyde columns from the Ozone Monitoring Instrument:  
529 Urban versus background levels and evaluation using aircraft data and a global model, *Journal of*  
530 *Geophysical Research: Atmospheres*, 116, doi:10.1029/2010JD014870, 2011.
- 531 Brent, L. C., Thorn, W. J., Gupta, M., Leen, B., Stehr, J. W., He, H., Arkinson, H. L., Weinheimer, A., Garland, C.,  
532 Pusede, S. E., Wooldridge, P. J., Cohen, R. C., and Dickerson, R. R.: Evaluation of the use of a  
533 commercially available cavity ringdown absorption spectrometer for measuring NO<sub>2</sub> in flight, and  
534 observations over the Mid-Atlantic States, during DISCOVER-AQ, *Journal of Atmospheric Chemistry*, 1-  
535 19, 10.1007/s10874-013-9265-6, 2013.
- 536 Cambaliza, M. O. L., Shepson, P. B., Caulton, D. R., Stirm, B., Samarov, D., Gurney, K. R., Turnbull, J., Davis, K.  
537 J., Possolo, A., Karion, A., Sweeney, C., Moser, B., Hendricks, A., Lauvaux, T., Mays, K., Whetstone, J.,  
538 Huang, J., Razlivanov, I., Miles, N. L., and Richardson, S. J.: Assessment of uncertainties of an aircraft-  
539 based mass balance approach for quantifying urban greenhouse gas emissions, *Atmospheric Chemistry and*



- Physics, 14, 9029-9050, 10.5194/acp-14-9029-2014, 2014.
- Canty, T. P., Hembeck, L., Vinciguerra, T. P., Anderson, D. C., Goldberg, D. L., Carpenter, S. F., Allen, D. J., Loughner, C. P., Salawitch, R. J., and Dickerson, R. R.: Ozone and NO<sub>x</sub> chemistry in the eastern US: evaluation of CMAQ/CB05 with satellite (OMI) data, *Atmospheric Chemistry and Physics*, 15, 10965-10982, 10.5194/acp-15-10965-2015, 2015.
- Castellanos, P., Luke, W. T., Kelley, P., Stehr, J. W., Ehrman, S. H., and Dickerson, R. R.: Modification of a commercial cavity ring-down spectroscopy NO<sub>2</sub> detector for enhanced sensitivity, *Review of Scientific Instruments*, 80, 113107, 10.1063/1.3244090, 2009.
- Chameides, W. L., Li, X. S., Tang, X. Y., Zhou, X. J., Luo, C., Kiang, C. S., St John, J., Saylor, R. D., Liu, S. C., Lam, K. S., Wang, T., and Giorgi, F.: Is ozone pollution affecting crop yields in China?, *Geophysical Research Letters*, 26, 867-870, 10.1029/1999gl1900068, 1999.
- Chan, C. K., and Yao, X.: Air pollution in mega cities in China, *Atmospheric Environment*, 42, 1-42, 10.1016/j.atmosenv.2007.09.003, 2008.
- Chance, K.: OMI/Aura Formaldehyde (HCHO) Total Column 1-orbit L2 Swath 13x24 km V003, Greenbelt, MD, USA, Goddard Earth Sciences Data and Information Services Center (GES DISC), Accessed: January 2018, 10.5067/Aura/OMI/DATA2015, 2007.
- Chen, Y. Y., Ebenstein, A., Greenstone, M., and Li, H. B.: Evidence on the impact of sustained exposure to air pollution on life expectancy from China's Huai River policy, *Proc. Natl. Acad. Sci. U. S. A.*, 110, 12936-12941, 10.1073/pnas.1300018110, 2013.
- Chou, C. C. K., Tsai, C.-Y., Shiu, C.-J., Liu, S. C., and Zhu, T.: Measurement of NO<sub>y</sub> during Campaign of Air Quality Research in Beijing 2006 (CAREBeijing-2006): Implications for the ozone production efficiency of NO<sub>x</sub>, *Journal of Geophysical Research-Atmospheres*, 114, D00g01, 10.1029/2008jd010446, 2009.
- Clough, S. A., Shephard, M. W., Mlawer, E. J., Delamere, J. S., Iacono, M. J., Cady-Pereira, K., Boukabara, S., and Brown, P. D.: Atmospheric radiative transfer modeling: a summary of the AER codes, *Journal of Quantitative Spectroscopy and Radiative Transfer*, 91, 233-244, <https://doi.org/10.1016/j.jqsrt.2004.05.058>, 2005.
- Crutzen, P. J.: Photochemical reactions initiated by and influencing ozone in unpolluted tropospheric air, *Tellus*, 26, 47-57, 1974.
- de Foy, B., Lu, Z., Streets, D. G., Lamsal, L. N., and Duncan, B. N.: Estimates of power plant NO<sub>x</sub> emissions and lifetimes from OMI NO<sub>2</sub> satellite retrievals, *Atmospheric Environment*, 116, 1-11, <http://dx.doi.org/10.1016/j.atmosenv.2015.05.056>, 2015.
- Dee, D. P., Uppala, S. M., Simmons, A. J., Berrisford, P., Poli, P., Kobayashi, S., Andrae, U., Balmaseda, M. A., Balsamo, G., Bauer, P., Bechtold, P., Beljaars, A. C. M., van de Berg, L., Bidlot, J., Bormann, N., Delsol, C., Dragani, R., Fuentes, M., Geer, A. J., Haimberger, L., Healy, S. B., Hersbach, H., Hólm, E. V., Isaksen, I., Kållberg, P., Köhler, M., Matricardi, M., McNally, A. P., Monge-Sanz, B. M., Morcrette, J. J., Park, B. K., Peubey, C., de Rosnay, P., Tavolato, C., Thépaut, J. N., and Vitart, F.: The ERA-Interim reanalysis: configuration and performance of the data assimilation system, *Q. J. R. Meteorol. Soc.*, 137, 553-597, 10.1002/qj.828, 2011.
- Deeter, M. N., Emmons, L. K., Francis, G. L., Edwards, D. P., Gille, J. C., Warner, J. X., Khattatov, B., Ziskin, D., Lamarque, J. F., Ho, S. P., Yudin, V., Attie, J. L., Packman, D., Chen, J., Mao, D., and Drummond, J. R.: Operational carbon monoxide retrieval algorithm and selected results for the MOPITT instrument, *Journal of Geophysical Research-Atmospheres*, 108, 4399, 10.1029/2002jd003186, 2003.
- Deeter, M. N., Worden, H. M., Edwards, D. P., Gille, J. C., and Andrews, A. E.: Evaluation of MOPITT retrievals of lower-tropospheric carbon monoxide over the United States, *Journal of Geophysical Research-Atmospheres*, 117, D13306, 10.1029/2012jd017553, 2012.
- Derwent, R. G., Stevenson, D. S., Collins, W. J., and Johnson, C. E.: Intercontinental transport and the origins of the ozone observed at surface sites in Europe, *Atmospheric Environment*, 38, 1891-1901, 10.1016/j.atmosenv.2004.01.008, 2004.
- Dickerson, R. R., Li, C., Li, Z., Marufu, L. T., Stehr, J. W., McClure, B., Krotkov, N., Chen, H., Wang, P., Xia, X., Ban, X., Gong, F., Yuan, J., and Yang, J.: Aircraft observations of dust and pollutants over northeast China: Insight into the meteorological mechanisms of transport, *Journal of Geophysical Research-Atmospheres*, 112, D24s90, 10.1029/2007jd008999, 2007.
- Ding, K., Liu, J., Ding, A., Liu, Q., Zhao, T. L., Shi, J., Han, Y., Wang, H., and Jiang, F.: Uplifting of carbon monoxide from biomass burning and anthropogenic sources to the free troposphere in East Asia, *Atmospheric Chemistry and Physics*, 15, 2843-2866, 10.5194/acp-15-2843-2015, 2015.
- Dodge, M.: Chemistry of Oxidant Formation: Implications for Designing Effective Control Strategies U.S.



- Environmental Protection Agency, Washington, D.C. EPA/600/D-87/114 (NTIS PB87179990), 1987.
- Duncan, B. N., Yoshida, Y., Olson, J. R., Sillman, S., Martin, R. V., Lamsal, L., Hu, Y. T., Pickering, K. E., Retscher, C., Allen, D. J., and Crawford, J. H.: Application of OMI observations to a space-based indicator of NO<sub>x</sub> and VOC controls on surface ozone formation, *Atmospheric Environment*, 44, 2213-2223, 10.1016/j.atmosenv.2010.03.010, 2010.
- Duncan, B. N., Lamsal, L. N., Thompson, A. M., Yoshida, Y., Lu, Z. F., Streets, D. G., Hurwitz, M. M., and Pickering, K. E.: A space-based, high-resolution view of notable changes in urban NO<sub>x</sub> pollution around the world (2005-2014), *Journal of Geophysical Research-Atmospheres*, 121, 976-996, 10.1002/2015jd024121, 2016.
- EPA: CMAQ (Version 5.2) Scientific Document, Zenodo. <https://doi.org/10.5281/zenodo.1167892>, 2017.
- European Commission: Joint Research Centre (JRC)/Netherlands Environmental Assessment Agency (PBL). Emission Database for Global Atmospheric Research (EDGAR), release version 4.2., available at: <http://edgar.jrc.ec.europa.eu> (accessed in March 2017), 2011.
- Fang, M., Chan, C. K., and Yao, X. H.: Managing air quality in a rapidly developing nation: China, *Atmospheric Environment*, 43, 79-86, 10.1016/j.atmosenv.2008.09.064, 2009.
- Finlayson-Pitts, B. J., and Pitts, J. N.: *Chemistry of the Upper and Lower Atmosphere*, 1st ed., Academic Press, UK, 1999.
- Fishman, J., Solomon, S., and Crutzen, P. J.: Observational and theoretical evidence in support of a significant insitu photo-chemical source of tropospheric ozone, *Tellus*, 31, 432-446, 1979.
- Gilpin, T., Apel, E., Fried, A., Wert, B., Calvert, J., Genfa, Z., Dasgupta, P., Harder, J. W., Heikes, B., Hopkins, B., Westberg, H., Kleindienst, T., Lee, Y.-N., Zhou, X., Lonneman, W., and Sewell, S.: Intercomparison of six ambient [CH<sub>2</sub>O] measurement techniques, *Journal of Geophysical Research: Atmospheres*, 102, 21161-21188, 10.1029/97jd01314, 1997.
- Goldberg, D. L., Vinciguerra, T. P., Anderson, D. C., Hembeck, L., Canty, T. P., Ehrman, S. H., Martins, D. K., Stauffer, R. M., Thompson, A. M., Salawitch, R. J., and Dickerson, R. R.: CAMx Ozone Source Attribution in the Eastern United States using Guidance from Observations during DISCOVER-AQ Maryland, *Geophysical Research Letters*, 2015GL067332, 10.1002/2015gl067332, 2016.
- González Abad, G., Liu, X., Chance, K., Wang, H., Kurosu, T. P., and Suleiman, R.: Updated Smithsonian Astrophysical Observatory Ozone Monitoring Instrument (SAO OMI) formaldehyde retrieval, *Atmos. Meas. Tech.*, 8, 19-32, 10.5194/amt-8-19-2015, 2015.
- Gu, D. S., Wang, Y. H., Smeltzer, C., and Liu, Z.: Reduction in NO<sub>x</sub> Emission Trends over China: Regional and Seasonal Variations, *Environmental Science & Technology*, 47, 12912-12919, 10.1021/es401727e, 2013.
- Guan, D. B., Meng, J., Reiner, D. M., Zhang, N., Shan, Y. L., Mi, Z. F., Shao, S., Liu, Z., Zhang, Q., and Davis, S. J.: Structural decline in China's CO<sub>2</sub> emissions through transitions in industry and energy systems, *Nature Geoscience*, 11, 551-+, 10.1038/s41561-018-0161-1, 2018.
- Guo, J., Miao, Y., Zhang, Y., Liu, H., Li, Z., Zhang, W., He, J., Lou, M., Yan, Y., Bian, L., and Zhai, P.: The climatology of planetary boundary layer height in China derived from radiosonde and reanalysis data, *Atmos. Chem. Phys.*, 16, 13309-13319, 10.5194/acp-16-13309-2016, 2016.
- Haagensmit, A. J.: Chemistry and physiology of Los-Angeles smog, *Industrial and Engineering Chemistry*, 44, 1342-1346, 10.1021/ie50510a045, 1952.
- Hains, J. C., Taubman, B. F., Thompson, A. M., Stehr, J. W., Marufu, L. T., Doddridge, B. G., and Dickerson, R. R.: Origins of chemical pollution derived from Mid-Atlantic aircraft profiles using a clustering technique, *Atmospheric Environment*, 42, 1727-1741, 10.1016/j.atmosenv.2007.11.052, 2008.
- Halliday, H. S., DiGangi, J. P., Choi, Y., Diskin, G. S., Pusede, S. E., Rana, M., Nowak, J. B., Knote, C., Ren, X., He, H., Dickerson, R. R., and Li, Z.: Using Short-Term CO/CO<sub>2</sub> Ratios to Assess Airmass Differences over the Korean Peninsula during KORUS-AQ *Journal of Geophysical Research: Atmospheres*, to be submitted, 2018.
- He, H., Li, C., Loughner, C. P., Li, Z., Krotkov, N. A., Yang, K., Wang, L., Zheng, Y., Bao, X., Zhao, G., and Dickerson, R. R.: SO<sub>2</sub> over central China: Measurements, numerical simulations and the tropospheric sulfur budget, *Journal of Geophysical Research: Atmospheres*, 117, doi:10.1029/2011JD016473, 2012.
- He, H., Loughner, C. P., Stehr, J. W., Arkinson, H. L., Brent, L. C., Follette-Cook, M. B., Tzortziou, M. A., Pickering, K. E., Thompson, A. M., Martins, D. K., Diskin, G. S., Anderson, B. E., Crawford, J. H., Weinheimer, A. J., Lee, P., Hains, J. C., and Dickerson, R. R.: An elevated reservoir of air pollutants over the Mid-Atlantic States during the 2011 DISCOVER-AQ campaign: Airborne measurements and numerical simulations, *Atmospheric Environment*, 85, 18-30, 10.1016/j.atmosenv.2013.11.039, 2014.
- He, K. B., Yang, F. M., Ma, Y. L., Zhang, Q., Yao, X. H., Chan, C. K., Cadle, S., Chan, T., and Mulawa, P.: The



- characteristics of PM<sub>2.5</sub> in Beijing, China, *Atmospheric Environment*, 35, 4959-4970, 10.1016/s1352-2310(01)00301-6, 2001.
- Heimbürger, A. M. F., Harvey, R. M., Shepson, P. B., Stirn, B. H., Gore, C., Turnbull, J., Cambaliza, M. O. L., Salmon, O. E., Kerlo, A. E. M., Lavoie, T. N., Davis, K. J., Lauvaux, T., Karion, A., Sweeney, C., Brewer, W. A., Hardesty, R. M., and Gurney, K. R.: Assessing the optimized precision of the aircraft mass balance method for measurement of urban greenhouse gas emission rates through averaging, *Elementa-Science of the Anthropocene*, 5, 26, 10.1525/elementa.134, 2017.
- Hong, S.-Y., and Lim, J.-O.: The WRF single-moment 6-class microphysics scheme (WSM6), *J. Korean Meteor. Soc.*, 42, 129-151, 2006.
- Huang, J., Liu, H., Crawford, J. H., Chan, C., Considine, D. B., Zhang, Y., Zheng, X., Zhao, C., Thouret, V., Oltmans, S. J., Liu, S. C., Jones, D. B. A., Steenrod, S. D., and Damon, M. R.: Origin of springtime ozone enhancements in the lower troposphere over Beijing: in situ measurements and model analysis, *Atmospheric Chemistry and Physics*, 15, 5161-5179, 10.5194/acp-15-5161-2015, 2015.
- IPCC: Climate Change 2014: Synthesis Report. Contribution of Working Groups I, II and III to the Fifth Assessment Report of the Intergovernmental Panel on Climate Change [Core Writing Team, R.K. Pachauri and L.A. Meyer (eds.)], IPCC, Geneva, Switzerland, 151 pp., 2014.
- Jacob, D. J., Logan, J. A., and Murti, P. P.: Effect of rising Asian emissions on surface ozone in the United States, *Geophysical Research Letters*, 26, 2175-2178, 10.1029/1999gl900450, 1999.
- Jerrett, M., Burnett, R. T., Pope, C. A., Ito, K., Thurston, G., Krewski, D., Shi, Y. L., Calle, E., and Thun, M.: Long-Term Ozone Exposure and Mortality, *N. Engl. J. Med.*, 360, 1085-1095, 10.1056/NEJMoa0803894, 2009.
- Jiang, Z., Worden, J. R., Jones, D. B. A., Lin, J. T., Verstraeten, W. W., and Henze, D. K.: Constraints on Asian ozone using Aura TES, OMI and Terra MOPITT, *Atmospheric Chemistry and Physics*, 15, 99-112, 10.5194/acp-15-99-2015, 2015.
- Jin, X., and Holloway, T.: Spatial and temporal variability of ozone sensitivity over China observed from the Ozone Monitoring Instrument, *Journal of Geophysical Research: Atmospheres*, 120, 7229-7246, doi:10.1002/2015JD023250, 2015.
- Jin, X., Fiore, A. M., Murray, L. T., Valin, L. C., Lamsal, L. N., Duncan, B., Folkert Boersma, K., De Smedt, I., Abad, G. G., Chance, K., and Tonnesen, G. S.: Evaluating a Space-Based Indicator of Surface Ozone-NO<sub>x</sub>-VOC Sensitivity Over Midlatitude Source Regions and Application to Decadal Trends, *Journal of Geophysical Research: Atmospheres*, 122, 10,439-410,461, doi:10.1002/2017JD026720, 2017.
- Kain, J. S.: The Kain-Fritsch convective parameterization: An update, *Journal of Applied Meteorology*, 43, 170-181, 2004.
- Kan, H. D., Chen, R. J., and Tong, S. L.: Ambient air pollution, climate change, and population health in China, *Environ. Int.*, 42, 10-19, 10.1016/j.envint.2011.03.003, 2012.
- Kleinman, L. I.: Low and high NO<sub>x</sub> tropospheric photochemistry, *Journal of Geophysical Research-Atmospheres*, 99, 16831-16838, 10.1029/94jd01028, 1994.
- Kleinman, L. I.: Ozone process insights from field experiments - part II: Observation-based analysis for ozone production, *Atmospheric Environment*, 34, 2023-2033, 10.1016/s1352-2310(99)00457-4, 2000.
- Krotkov, N. A., McLinden, C. A., Li, C., Lamsal, L. N., Celarier, E. A., Marchenko, S. V., Swartz, W. H., Bucsela, E. J., Joiner, J., Duncan, B. N., Boersma, K. F., Veefkind, J. P., Levelt, P. F., Fioletov, V. E., Dickerson, R. R., He, H., Lu, Z. F., and Streets, D. G.: Aura OMI observations of regional SO<sub>2</sub> and NO<sub>2</sub> pollution changes from 2005 to 2015, *Atmospheric Chemistry and Physics*, 16, 4605-4629, 10.5194/acp-16-4605-2016, 2016.
- Krotkov, N. A., Lamsal, L. N., Celarier, E. A., Swartz, W. H., Marchenko, S. V., Bucsela, E. J., Chan, K. L., Wenig, M., and Zara, M.: The version 3 OMI NO<sub>2</sub> standard product, *Atmos. Meas. Tech.*, 10, 3133-3149, 10.5194/amt-10-3133-2017, 2017.
- Krotkov, N. A., Lamsal, L. N., Marchenko, S. V., Celarier, E. A., Bucsela, E. J., Swartz, W. H., and Veefkind, J. P.: OMI/Aura Nitrogen Dioxide (NO<sub>2</sub>) Total and Tropospheric Column 1-orbit L2 Swath 13x24 km V003, Greenbelt, MD, USA, Goddard Earth Sciences Data and Information Services Center (GES DISC), Accessed: January 2018, 10.5067/Aura/OMI/DATA2017, 2018.
- Kurokawa, J., Ohara, T., Morikawa, T., Hanayama, S., Janssens-Maenhout, G., Fukui, T., Kawashima, K., and Akimoto, H.: Emissions of air pollutants and greenhouse gases over Asian regions during 2000-2008: Regional Emission inventory in ASia (REAS) version 2, *Atmospheric Chemistry and Physics*, 13, 11019-11058, 10.5194/acp-13-11019-2013, 2013.
- Lacis, A. A., Wuebbles, D. J., and Logan, J. A.: Radiative forcing of climate by changes in the vertical-distribution of ozone, *Journal of Geophysical Research-Atmospheres*, 95, 9971-9981, 10.1029/JD09SiD07p09971, 1990.





- 708 Lelieveld, J., Evans, J. S., Fnais, M., Giannadaki, D., and Pozzer, A.: The contribution of outdoor air pollution  
709 sources to premature mortality on a global scale, *Nature*, 525, 367–+, 10.1038/nature15371, 2015.
- 710 Levelt, P. F., Hilsenrath, E., Leppelmeier, G. W., van den Oord, G. H. J., Bhartia, P. K., Tamminen, J., de Haan, J. F.,  
711 and Veefkind, J. P.: Science objectives of the Ozone Monitoring Instrument, *Ieee Transactions on*  
712 *Geoscience and Remote Sensing*, 44, 1199–1208, 10.1109/tgrs.2006.872336, 2006.
- 713 Li, M., Zhang, Q., Kurokawa, J., Woo, J. H., He, K. B., Lu, Z. F., Ohara, T., Song, Y., Streets, D. G., Carmichael, G.  
714 R., Cheng, Y. F., Hong, C. P., Huo, H., Jiang, X. J., Kang, S. C., Liu, F., Su, H., and Zheng, B.: MIX: a  
715 mosaic Asian anthropogenic emission inventory under the international collaboration framework of the  
716 MICS-Asia and HTAP, *Atmospheric Chemistry and Physics*, 17, 935–963, 10.5194/acp-17-935-2017,  
717 2017a.
- 718 Li, Z., Guo, J., Ding, A., Liao, H., Liu, J., Sun, Y., Wang, T., Xue, H., Zhang, H., and Zhu, B.: Aerosol and  
719 boundary-layer interactions and impact on air quality, *National Science Review*, 4, 810–833,  
720 10.1093/nsr/nwx117, 2017b.
- 721 Lin, J., Nielsen, C. P., Zhao, Y., Lei, Y., Liu, Y., and McElroy, M. B.: Recent Changes in Particulate Air Pollution  
722 over China Observed from Space and the Ground: Effectiveness of Emission Control, *Environmental*  
723 *Science & Technology*, 44, 7771–7776, 10.1021/es101094t, 2010a.
- 724 Lin, J. T., Wuebbles, D. J., and Liang, X. Z.: Effects of intercontinental transport on surface ozone over the United  
725 States: Present and future assessment with a global model, *Geophysical Research Letters*, 35, L02805,  
726 10.1029/2007gl031415, 2008.
- 727 Lin, J. T., McElroy, M. B., and Boersma, K. F.: Constraint of anthropogenic NO<sub>x</sub> emissions in China from different  
728 sectors: a new methodology using multiple satellite retrievals, *Atmospheric Chemistry and Physics*, 10, 63–  
729 78, 10.5194/acp-10-63-2010, 2010b.
- 730 Liu, F., Zhang, Q., Ronald, J. V., Zheng, B., Tong, D., Yan, L., Zheng, Y. X., and He, K. B.: Recent reduction in NO<sub>x</sub>  
731 emissions over China: synthesis of satellite observations and emission inventories, *Environ. Res. Lett.*, 11,  
732 114002, 10.1088/1748-9326/11/11/114002, 2016.
- 733 Logan, J. A., Prather, M. J., Wofsy, S. C., and McElroy, M. B.: Tropospheric chemistry - a global perspective,  
734 *Journal of Geophysical Research-Oceans and Atmospheres*, 86, 7210–7254, 10.1029/JC086iC08p07210,  
735 1981.
- 736 Mazzuca, G. M., Ren, X. R., Loughner, C. P., Estes, M., Crawford, J. H., Pickering, K. E., Weinheimer, A. J., and  
737 Dickerson, R. R.: Ozone production and its sensitivity to NO<sub>x</sub> and VOCs: results from the DISCOVER-AQ  
738 field experiment, Houston 2013, *Atmospheric Chemistry and Physics*, 16, 14463–14474, 10.5194/acp-16-  
739 14463-2016, 2016.
- 740 Millet, D. B., Jacob, D. J., Turquety, S., Hudman, R. C., Wu, S., Fried, A., Walega, J., Heikes, B. G., Blake, D. R.,  
741 Singh, H. B., Anderson, B. E., and Clarke, A. D.: Formaldehyde distribution over North America:  
742 Implications for satellite retrievals of formaldehyde columns and isoprene emission, *Journal of Geophysical*  
743 *Research: Atmospheres*, 111, doi:10.1029/2005JD006853, 2006.
- 744 MOPITT Science Team: MOPITT/Terra Level 3 Gridded Daily CO (on a latitude/longitude/pressure grid) derived  
745 from Near and Thermal Infrared Radiances, version 7, Hampton, VA, USA: NASA Atmospheric Science  
746 Data Center (ASDC), Accessed January 2018, 10.5067/TERRA/MOPITT/MOP03J\_L3.007, 2013.
- 747 Ni, R. J., Lin, J. T., Yan, Y. Y., and Lin, W. L.: Foreign and domestic contributions to springtime ozone over China,  
748 *Atmospheric Chemistry and Physics*, 18, 11447–11469, 10.5194/acp-18-11447-2018, 2018.
- 749 Ohara, T., Akimoto, H., Kurokawa, J., Horii, N., Yamaji, K., Yan, X., and Hayasaka, T.: An Asian emission  
750 inventory of anthropogenic emission sources for the period 1980–2020, *Atmospheric Chemistry and*  
751 *Physics*, 7, 4419–4444, 10.5194/acp-7-4419-2007, 2007.
- 752 Pleim, J. E., and Xiu, A.: Development and Testing of a Surface Flux and Planetary Boundary Layer Model for  
753 Application in Mesoscale Models, *Journal of Applied Meteorology*, 34, 16–32, 10.1175/1520-0450-34.1.16,  
754 1995.
- 755 Pleim, J. E.: A Combined Local and Nonlocal Closure Model for the Atmospheric Boundary Layer. Part I: Model  
756 Description and Testing, *J. Appl. Meteorol. Climatol.*, 46, 1383–1395, 10.1175/jam2539.1, 2007.
- 757 Qu, Z., Henze, D. K., Capps, S. L., Wang, Y., Xu, X. G., Wang, J., and Keller, M.: Monthly top-down NO<sub>x</sub>  
758 emissions for China (2005–2012): A hybrid inversion method and trend analysis, *Journal of Geophysical*  
759 *Research-Atmospheres*, 122, 4600–4625, 10.1002/2016jd025852, 2017.
- 760 Ramanathan, V., and Dickinson, R. E.: Role of stratospheric ozone in the zonal and seasonal radiative energy-  
761 balance of the Earth-troposphere system, *Journal of the Atmospheric Sciences*, 36, 1084–1104, 1979.
- 762 Rappenglück, B., Dasgupta, P. K., Leuchner, M., Li, Q., and Luke, W.: Formaldehyde and its relation to CO, PAN,  
763 and SO<sub>2</sub> in the Houston-Galveston airshed, *Atmos. Chem. Phys.*, 10, 2413–2424,



- 10.5194/acp-10-2413-2010, 2010.
- Ren, X., Salmon, O. E., Hansford, J. R., Ahn, D., Hall, D., Benish, S. E., Stratton, P. R., He, H., Sahu, S., Grimes, C., Heimburger, A. M. F., Martin, C. R., Cohen, M. D., Stunder, B., Salawitch, R. J., Ehrman, S. H., Shepson, P. B., and Dickerson, R. R.: Methane Emissions From the Baltimore-Washington Area Based on Airborne Observations: Comparison to Emissions Inventories, *Journal of Geophysical Research: Atmospheres*, 0, doi:10.1029/2018JD028851, 2018.
- Ring, A. M., Canty, T. P., Anderson, D. C., Vinciguerra, T. P., He, H., Goldberg, D. L., Ehrman, S. H., Dickerson, R. R., and Salawitch, R. J.: Evaluating commercial marine emissions and their role in air quality policy using observations and the CMAQ model, *Atmospheric Environment*, 173, 96-107, <https://doi.org/10.1016/j.atmosenv.2017.10.037>, 2018.
- Salmon, O. E., Shepson, P. B., Ren, X., He, H., Hall, D. L., Dickerson, R. R., Stirm, B. H., Brown, S. S., Fibiger, D. L., McDuffie, E. E., Campos, T. L., Gurney, K. R., and Thornton, J. A.: Top-Down Estimates of NO<sub>x</sub> and CO Emissions From Washington, D.C.-Baltimore During the WINTER Campaign, *Journal of Geophysical Research: Atmospheres*, 123, 7705-7724, doi:10.1029/2018JD028539, 2018.
- Schroeder, J. R., Crawford, J. H., Fried, A., Walega, J., Weinheimer, A., Wisthaler, A., Muller, M., Mikoviny, T., Chen, G., Shook, M., Blake, D. R., and Tonnesen, G. S.: New insights into the column CH<sub>2</sub>O/NO<sub>2</sub> ratio as an indicator of near-surface ozone sensitivity, *Journal of Geophysical Research-Atmospheres*, 122, 8885-8907, 10.1002/2017jd026781, 2017.
- Seinfeld, J. H., and Pandis, S. N.: *Atmospheric Chemistry and Physics: From Air Pollution to Climate Change*, 2nd ed., John Wiley & Sons, Inc., 2006.
- Shan, Y., Guan, D., Zheng, H., Ou, J., Li, Y., Meng, J., Mi, Z., Liu, Z., and Zhang, Q.: China CO<sub>2</sub> emission accounts 1997–2015, *Scientific Data*, 5, 170201, 10.1038/sdata.2017.201, <https://www.nature.com/articles/sdata2017201#supplementary-information>, 2018.
- Sillman, S.: The relation between ozone, NO<sub>x</sub> and hydrocarbons in urban and polluted rural environments, *Atmospheric Environment*, 33, 1821-1845, 10.1016/s1352-2310(98)00345-8, 1999.
- Skamarock, W. C., Klemp, J. B., Dudhia, J., Gill, D. O., Barker, D. M., Duda, M. G., Huang, X.-Y., Wang, W., and Powers, J. G.: A Description of the Advanced Research WRF Version 3, NCAR Technical Note, NCAR/TN-475+STR, 113 pp, 2008.
- Stavrakou, T., Muller, J. F., Bauwens, M., De Smedt, I., Lerot, C., Van Roozendaal, M., Coheur, P. F., Clerbaux, C., Boersma, K. F., van der A, R., and Song, Y.: Substantial Underestimation of Post-Harvest Burning Emissions in the North China Plain Revealed by Multi-Species Space Observations, *Scientific Reports*, 6, 32307, 10.1038/srep32307, 2016.
- Stevenson, D. S., Dentener, F. J., Schultz, M. G., Ellingsen, K., van Noije, T. P. C., Wild, O., Zeng, G., Amann, M., Atherton, C. S., Bell, N., Bergmann, D. J., Bey, I., Butler, T., Cofala, J., Collins, W. J., Derwent, R. G., Doherty, R. M., Drevet, J., Eskes, H. J., Fiore, A. M., Gauss, M., Hauglustaine, D. A., Horowitz, L. W., Isaksen, I. S. A., Krol, M. C., Lamarque, J. F., Lawrence, M. G., Montanaro, V., Muller, J. F., Pitari, G., Prather, M. J., Pyle, J. A., Rast, S., Rodriguez, J. M., Sanderson, M. G., Savage, N. H., Shindell, D. T., Strahan, S. E., Sudo, K., and Szopa, S.: Multimodel ensemble simulations of present-day and near-future tropospheric ozone, *Journal of Geophysical Research-Atmospheres*, 111, D08301, 10.1029/2005jd006338, 2006.
- Streets, D. G., Bond, T. C., Carmichael, G. R., Fernandes, S. D., Fu, Q., He, D., Klimont, Z., Nelson, S. M., Tsai, N. Y., Wang, M. Q., Woo, J. H., and Yarber, K. F.: An inventory of gaseous and primary aerosol emissions in Asia in the year 2000, *Journal of Geophysical Research-Atmospheres*, 108, 8809, 10.1029/2002jd003093, 2003.
- Sun, Y. L., Zhuang, G. S., Tang, A. H., Wang, Y., and An, Z. S.: Chemical characteristics of PM<sub>2.5</sub> and PM<sub>10</sub> in haze-fog episodes in Beijing, *Environmental Science & Technology*, 40, 3148-3155, 10.1021/es051533g, 2006.
- Taubman, B. F., Hains, J. C., Thompson, A. M., Marufu, L. T., Doddridge, B. G., Stehr, J. W., Piety, C. A., and Dickerson, R. R.: Aircraft vertical profiles of trace gas and aerosol pollution over the mid-Atlantic United States: Statistics and meteorological cluster analysis, *Journal of Geophysical Research-Atmospheres*, 111, D10s07 10.1029/2005jd006196, 2006.
- Thompson, A. M.: The oxidizing capacity of the Earth's Atmosphere - probable past and future changes, *Science*, 256, 1157-1165, 10.1126/science.256.5060.1157, 1992.
- Tie, X. X., Wu, D., and Brasseur, G.: Lung cancer mortality and exposure to atmospheric aerosol particles in Guangzhou, China, *Atmospheric Environment*, 43, 2375-2377, 10.1016/j.atmosenv.2009.01.036, 2009.
- UNC: SMOKE v4.5 User's Manual, The Institute for the Environment, The University of North Carolina at Chapel





- Hill, 2017.
- Verstraeten, W. W., Neu, J. L., Williams, J. E., Bowman, K. W., Worden, J. R., and Boersma, K. F.: Rapid increases in tropospheric ozone production and export from China, *Nature Geoscience*, 8, 690–+, 10.1038/ngeo2493, 2015.
- Wang, F., Li, Z., Ren, X., Jiang, Q., He, H., Dickerson, R. R., Dong, X., and Lv, F.: Vertical distributions of aerosol optical properties during the spring 2016 ARIAs airborne campaign in the North China Plain, *Atmos. Chem. Phys.*, 18, 8995–9010, 10.5194/acp-18-8995-2018, 2018a.
- Wang, R., Xu, X. B., Jia, S. H., Ma, R. S., Ran, L., Deng, Z. Z., Lin, W. L., Wang, Y., and Ma, Z. Q.: Lower tropospheric distributions of O<sub>3</sub> and aerosol over Raoyang, a rural site in the North China Plain, *Atmospheric Chemistry and Physics*, 17, 3891–3903, 10.5194/acp-17-3891-2017, 2017a.
- Wang, S. W., Zhang, Q., Streets, D. G., He, K. B., Martin, R. V., Lamsal, L. N., Chen, D., Lei, Y., and Lu, Z.: Growth in NO<sub>x</sub> emissions from power plants in China: bottom-up estimates and satellite observations, *Atmospheric Chemistry and Physics*, 12, 4429–4447, 10.5194/acp-12-4429-2012, 2012.
- Wang, S. X., and Hao, J. M.: Air quality management in China: Issues, challenges, and options, *J. Environ. Sci.*, 24, 2–13, 10.1016/S1001-0742(11)60724-9, 2012.
- Wang, S. X., Xing, J., Zhao, B., Jang, C., and Hao, J. M.: Effectiveness of national air pollution control policies on the air quality in metropolitan areas of China, *J. Environ. Sci.*, 26, 13–22, 10.1016/S1001-0742(13)60381-2, 2014a.
- Wang, T., Xue, L. K., Brimblecombe, P., Lam, Y. F., Li, L., and Zhang, L.: Ozone pollution in China: A review of concentrations, meteorological influences, chemical precursors, and effects, *Science of the Total Environment*, 575, 1582–1596, 10.1016/j.scitotenv.2016.10.081, 2017b.
- Wang, Y., Zhuang, G. S., Tang, A. H., Yuan, H., Sun, Y. L., Chen, S. A., and Zheng, A. H.: The ion chemistry and the source of PM<sub>2.5</sub> aerosol in Beijing, *Atmospheric Environment*, 39, 3771–3784, 10.1016/j.atmosenv.2005.03.013, 2005.
- Wang, Y., Li, Z., Zhang, Y., Du, W., Zhang, F., Tan, H., Xu, H., Fan, T., Jin, X., Fan, X., Dong, Z., Wang, Q., and Sun, Y.: Characterization of aerosol hygroscopicity, mixing state, and CCN activity at a suburban site in the central North China Plain, *Atmos. Chem. Phys.*, 18, 11739–11752, 10.5194/acp-18-11739-2018, 2018b.
- Wang, Y. S., Yao, L., Wang, L. L., Liu, Z. R., Ji, D. S., Tang, G. Q., Zhang, J. K., Sun, Y., Hu, B., and Xin, J. Y.: Mechanism for the formation of the January 2013 heavy haze pollution episode over central and eastern China, *Sci. China-Earth Sci.*, 57, 14–25, 10.1007/s11430-013-4773-4, 2014b.
- Wei, W., Wang, S. X., Hao, J. M., and Cheng, S. Y.: Projection of anthropogenic volatile organic compounds (VOCs) emissions in China for the period 2010–2020, *Atmospheric Environment*, 45, 6863–6871, 10.1016/j.atmosenv.2011.01.013, 2011.
- WHO: Health aspects of air pollution with particulate matter, ozone and nitrogen dioxide, World Health Organisation, Bonn, 2003.
- Worden, H. M., Deeter, M. N., Edwards, D. P., Gille, J. C., Drummond, J. R., and Nedelec, P.: Observations of near-surface carbon monoxide from space using MOPITT multispectral retrievals, *Journal of Geophysical Research-Atmospheres*, 115, D18314, 10.1029/2010jd014242, 2010.
- Xing, J., Wang, S. X., Jang, C., Zhu, Y., and Hao, J. M.: Nonlinear response of ozone to precursor emission changes in China: a modeling study using response surface methodology, *Atmospheric Chemistry and Physics*, 11, 5027–5044, 10.5194/acp-11-5027-2011, 2011.
- Xing, J., Ding, D., Wang, S. X., Zhao, B., Jang, C., Wu, W. J., Zhang, F. F., Zhu, Y., and Hao, J. M.: Quantification of the enhanced effectiveness of NO<sub>x</sub> control from simultaneous reductions of VOC and NH<sub>3</sub> for reducing air pollution in the Beijing-Tianjin-Hebei region, China, *Atmospheric Chemistry and Physics*, 18, 7799–7814, 10.5194/acp-18-7799-2018, 2018.
- Xiu, A., and Pleim, J. E.: Development of a Land Surface Model. Part I: Application in a Mesoscale Meteorological Model, *Journal of Applied Meteorology*, 40, 192–209, 10.1175/1520-0450(2001)040<0192:doalsm>2.0.co;2, 2001.
- Xue, L. K., Wang, T., Gao, J., Ding, A. J., Zhou, X. H., Blake, D. R., Wang, X. F., Saunders, S. M., Fan, S. J., Zuo, H. C., Zhang, Q. Z., and Wang, W. X.: Ground-level ozone in four Chinese cities: precursors, regional transport and heterogeneous processes, *Atmospheric Chemistry and Physics*, 14, 13175–13188, 10.5194/acp-14-13175-2014, 2014.
- Yang, F., Tan, J., Zhao, Q., Du, Z., He, K., Ma, Y., Duan, F., and Chen, G.: Characteristics of PM<sub>2.5</sub> speciation in representative megacities and across China, *Atmospheric Chemistry and Physics*, 11, 5207–5219, 10.5194/acp-11-5207-2011, 2011.
- Yarwood, G. S., Rao, S. T., Yocke, M., and Whitten, G. Z.: Updates to the Carbon Bond Chemical Mechanism:



- 876 CB05, ENVIRON International Corp, 2005.
- 877 Yarwood, G. S., Whitten, G. Z., Jung, J., Heo, G., and Allen, D.: Development, Evaluation and Testing of Version 6
- 878 of the Carbon Bond Chemical Mechanism (CB6),
- 879 [https://www.tceq.texas.gov/assets/public/implementation/air/am/contracts/reports/pm/5820784005FY1026-](https://www.tceq.texas.gov/assets/public/implementation/air/am/contracts/reports/pm/5820784005FY1026-20100922-environ-cb6.pdf)
- 880 [20100922-environ-cb6.pdf](https://www.tceq.texas.gov/assets/public/implementation/air/am/contracts/reports/pm/5820784005FY1026-20100922-environ-cb6.pdf), 2010.
- 881 Ye, B. M., Ji, X. L., Yang, H. Z., Yao, X. H., Chan, C. K., Cadle, S. H., Chan, T., and Mulawa, P. A.: Concentration
- 882 and chemical composition of PM<sub>2.5</sub> in Shanghai for a 1-year period, *Atmospheric Environment*, 37, 499-
- 883 510, Pii s1352-2310(02)00918-4, 10.1016/s1352-2310(02)00918-4, 2003.
- 884 Young, P. J., Archibald, A. T., Bowman, K. W., Lamarque, J. F., Naik, V., Stevenson, D. S., Tilmes, S., Voulgarakis,
- 885 A., Wild, O., Bergmann, D., Cameron-Smith, P., Cionni, I., Collins, W. J., Dalsoren, S. B., Doherty, R. M.,
- 886 Eyring, V., Faluvegi, G., Horowitz, L. W., Josse, B., Lee, Y. H., MacKenzie, I. A., Nagashima, T., Plummer,
- 887 D. A., Righi, M., Rumbold, S. T., Skeie, R. B., Shindell, D. T., Strode, S. A., Sudo, K., Szopa, S., and Zeng,
- 888 G.: Pre-industrial to end 21st century projections of tropospheric ozone from the Atmospheric Chemistry
- 889 and Climate Model Intercomparison Project (ACCMIP), *Atmospheric Chemistry and Physics*, 13, 2063-
- 890 2090, 10.5194/acp-13-2063-2013, 2013.
- 891 Zhang, J. N., Xiao, J. F., Chen, X. F., Liang, X. M., Fan, L. Y., and Ye, D. Q.: Allowance and allocation of industrial
- 892 volatile organic compounds emission in China for year 2020 and 2030, *J. Environ. Sci.*, 69, 155-165,
- 893 10.1016/j.jes.2017.10.003, 2018.
- 894 Zhang, R., Jing, J., Tao, J., Hsu, S. C., Wang, G., Cao, J., Lee, C. S. L., Zhu, L., Chen, Z., Zhao, Y., and Shen, Z.: Chemical characterization and source apportionment of PM<sub>2.5</sub> in Beijing: seasonal perspective,
- 895 *Atmospheric Chemistry and Physics*, 13, 7053-7074, 10.5194/acp-13-7053-2013, 2013.
- 896 Zhang, W., Zhu, T., Yang, W., Bai, Z., Sun, Y. L., Xu, Y., Yin, B., and Zhao, X.: Airborne measurements of gas and
- 897 particle pollutants during CAREBeijing-2008, *Atmospheric Chemistry and Physics*, 14, 301-316,
- 898 10.5194/acp-14-301-2014, 2014.
- 899
- 900 Zhang, X. P., and Cheng, X. M.: Energy consumption, carbon emissions, and economic growth in China, *Ecological*
- 901 *Economics*, 68, 2706-2712, 10.1016/j.ecolecon.2009.05.011, 2009.
- 902 Zhang, X. Y., Wang, Y. Q., Niu, T., Zhang, X. C., Gong, S. L., Zhang, Y. M., and Sun, J. Y.: Atmospheric aerosol
- 903 compositions in China: spatial/temporal variability, chemical signature, regional haze distribution and
- 904 comparisons with global aerosols, *Atmospheric Chemistry and Physics*, 12, 779-799, 10.5194/acp-12-779-
- 905 2012, 2012.
- 906 Zhao, B., Wang, S. X., Liu, H., Xu, J. Y., Fu, K., Klimont, Z., Hao, J. M., He, K. B., Cofala, J., and Amann, M.: NO<sub>x</sub>
- 907 emissions in China: historical trends and future perspectives, *Atmospheric Chemistry and Physics*, 13,
- 908 9869-9897, 10.5194/acp-13-9869-2013, 2013a.
- 909 Zhao, P. S., Dong, F., He, D., Zhao, X. J., Zhang, X. L., Zhang, W. Z., Yao, Q., and Liu, H. Y.: Characteristics of
- 910 concentrations and chemical compositions for PM<sub>2.5</sub> in the region of Beijing, Tianjin, and Hebei, China,
- 911 *Atmospheric Chemistry and Physics*, 13, 4631-4644, 10.5194/acp-13-4631-2013, 2013b.
- 912 Zhao, Y., Zhang, J., and Nielsen, C. P.: The effects of recent control policies on trends in emissions of anthropogenic
- 913 atmospheric pollutants and CO<sub>2</sub> in China, *Atmospheric Chemistry and Physics*, 13, 487-508, 10.5194/acp-
- 914 13-487-2013, 2013c.
- 915 Zhao, Y., Mao, P., Zhou, Y., Yang, Y., Zhang, J., Wang, S., Dong, Y., Xie, F., Yu, Y., and Li, W.: Improved provincial
- 916 emission inventory and speciation profiles of anthropogenic non-methane volatile organic compounds: a
- 917 case study for Jiangsu, China, *Atmos. Chem. Phys.*, 17, 7733-7756, 10.5194/acp-17-7733-2017, 2017.
- 918 Zheng, B., Chevallier, F., Ciais, P., Yin, Y., Deeter, M. N., Worden, H. M., Wang, Y. L., Zhang, Q., and He, K. B.: Rapid decline in carbon monoxide emissions and export from East Asia between years 2005 and 2016,
- 919 *Environ. Res. Lett.*, 13, 044007, 10.1088/1748-9326/aab2b3, 2018.
- 920
- 921 Zhu, Y., Zhang, J., Wang, J., Chen, W., Han, Y., Ye, C., Li, Y., Liu, J., Zeng, L., Wu, Y., Wang, X., Wang, W., Chen,
- 922 J., and Zhu, T.: Distribution and sources of air pollutants in the North China Plain based on on-road mobile
- 923 measurements, *Atmos. Chem. Phys.*, 16, 12551-12565, 10.5194/acp-16-12551-2016, 2016.
- 924
- 925

926 **Tables and Figures**

927

928 **Table 1.** List of CMAQ simulations with adjusted emissions based on satellite observations.  
929 Anthropogenic CO, NO<sub>x</sub>, and VOCs emissions were adjusted using MOPITT CO, OMI NO<sub>2</sub>, and  
930 OMI HCHO observations.

931

Run NO.	Experiment Name	Bio. VOCs	Anthro. CO	Anthro. NO <sub>x</sub>	Anthro. VOCs
1	CMAQ_baseline	BEIS	EDGAR	EDGAR	EDGAR
2	CMAQ_noBEIS	N/A	EDGAR	EDGAR	EDGAR
3	CMAQ_CO	BEIS	Adjusted	EDGAR	EDGAR
4	CMAQ_NO <sub>x</sub>	BEIS	EDGAR	Adjusted	EDGAR
5	CMAQ_VOCs	BEIS	EDGAR	EDGAR	Adjusted
6	CMAQ_All	BEIS	Adjusted	Adjusted	Adjusted

932

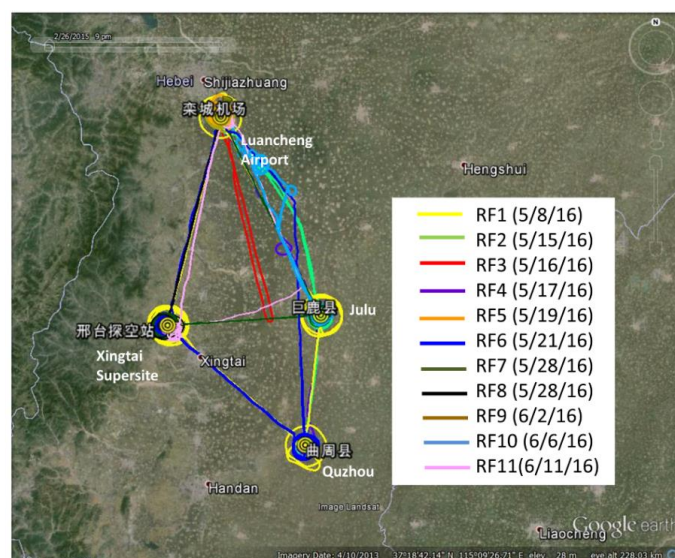


**Table 2.** Statistics of CMAQ performance of six sensitivity experiments compared with ARIAs aircraft measurements over the NCP.

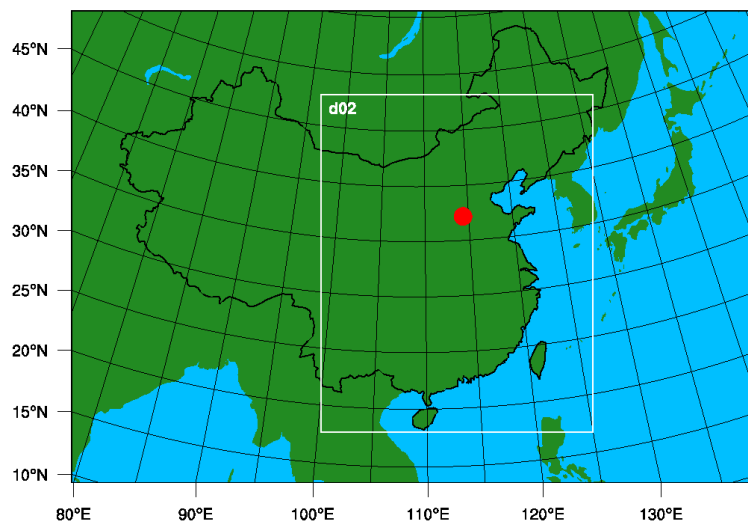
No	Name	Mean Diff	Slope	Stdev	Corr. R	NMB	NME	RMSE	Mean Ratio
		ppbv	Unitless	ppbv	Unitless	%	%	ppbv	Unitless
O <sub>3</sub>									
1	CMAQ_Baseline	-21.35	0.56	13.25	0.37	-25.14	25.86	25.10	0.75
2	CMAQ_noBEIS	-23.74	0.49	12.85	0.41	-27.94	28.34	26.97	0.72
3	CMAQ_NOx	-19.83	0.59	13.63	0.34	-23.34	24.18	24.03	0.77
4	CMAQ_VOCs	-19.26	0.66	13.66	0.36	-22.67	23.81	23.58	0.77
5	CMAQ_CO	-20.35	0.61	13.52	0.36	-23.96	24.83	24.40	0.76
6	CMAQ_All	-15.18	0.81	14.83	0.33	-17.87	20.33	21.18	0.82
CO									
1	CMAQ_Baseline	-183.56	0.21	165.92	0.23	-60.26	60.26	246.98	0.40
2	CMAQ_noBEIS	-186.34	0.21	165.52	0.25	-61.17	61.17	248.79	0.39
3	CMAQ_NOx	-184.25	0.21	165.76	0.24	-60.48	60.50	247.39	0.40
4	CMAQ_VOCs	-181.89	0.22	166.32	0.22	-59.71	59.78	246.01	0.40
5	CMAQ_CO	-148.55	0.36	167.90	0.22	-48.76	50.32	223.67	0.51
6	CMAQ_All	-104.45	0.52	175.48	0.21	-34.29	45.03	203.60	0.66
NO <sub>2</sub>									
1	CMAQ_Baseline	-1.72	0.31	3.09	0.58	-59.91	64.59	3.52	0.40
2	CMAQ_noBEIS	-1.73	0.31	3.09	0.58	-60.47	64.90	3.52	0.40
3	CMAQ_NOx	-1.45	0.38	2.99	0.60	-50.61	61.26	3.31	0.49
4	CMAQ_VOCs	-1.76	0.31	3.10	0.58	-61.60	65.66	3.55	0.38
5	CMAQ_CO	-1.70	0.31	3.09	0.58	-59.28	64.20	3.51	0.41
6	CMAQ_All	-1.47	0.38	3.01	0.59	-51.23	61.62	3.33	0.49
NO									
1	CMAQ_Baseline	-0.25	0.99	0.47	0.68	-32.23	45.4	0.53	0.68
2	CMAQ_noBEIS	-0.24	1.02	0.48	0.68	-31.09	45.66	0.54	0.69
3	CMAQ_NOx	-0.08	1.31	0.59	0.67	-9.75	50.01	0.59	0.90
4	CMAQ_VOCs	-0.30	0.89	0.45	0.68	-38.63	46.58	0.54	0.61
5	CMAQ_CO	-0.26	0.96	0.47	0.68	-33.08	45.26	0.53	0.67
6	CMAQ_All	-0.16	1.13	0.52	0.67	-20.31	45.46	0.54	0.80
NO <sub>y</sub>									
1	CMAQ_Baseline	-15.26	0.30	10.15	0.39	-77.58	77.58	18.27	0.22
2	CMAQ_noBEIS	-15.50	0.29	10.15	0.40	-78.81	78.81	18.47	0.21
3	CMAQ_NOx	-14.24	0.37	10.20	0.37	-72.39	72.39	17.46	0.28
4	CMAQ_VOCs	-15.23	0.30	10.16	0.39	-77.42	77.42	18.25	0.23
5	CMAQ_CO	-15.26	0.30	10.15	0.39	-77.56	77.56	18.27	0.22
6	CMAQ_All	-14.21	0.37	10.20	0.37	-72.26	72.26	17.44	0.28



**Figure 1.** ARIAs flights over the NCP and the WRF-CMAQ domains. Eleven Research Flights (RF) were conducted in May to Mid-June 2016. CMAQ has two domains, the coarse domain (d01, 36 km resolution) covering East Asia and the nested domain (d02, 12 km resolution) focusing on eastern China. a) Summary of flight routes; b) WRF-CMAQ modeling domain (the red dot represents the location of the Xingtai supersite).



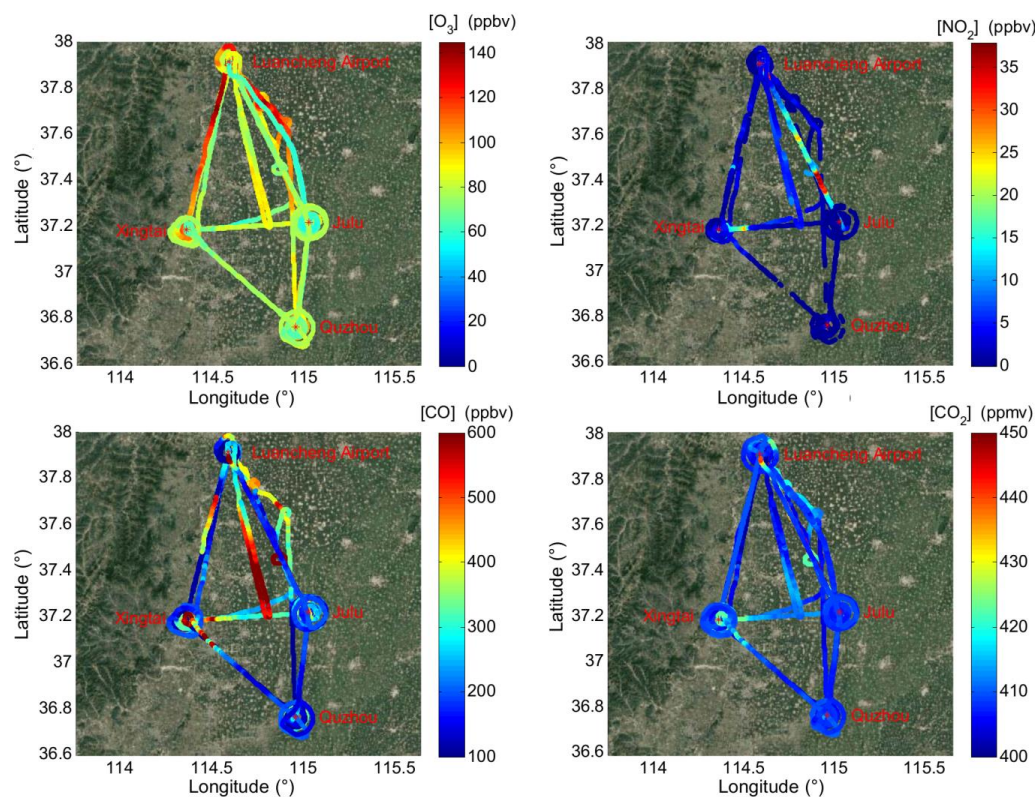
b)







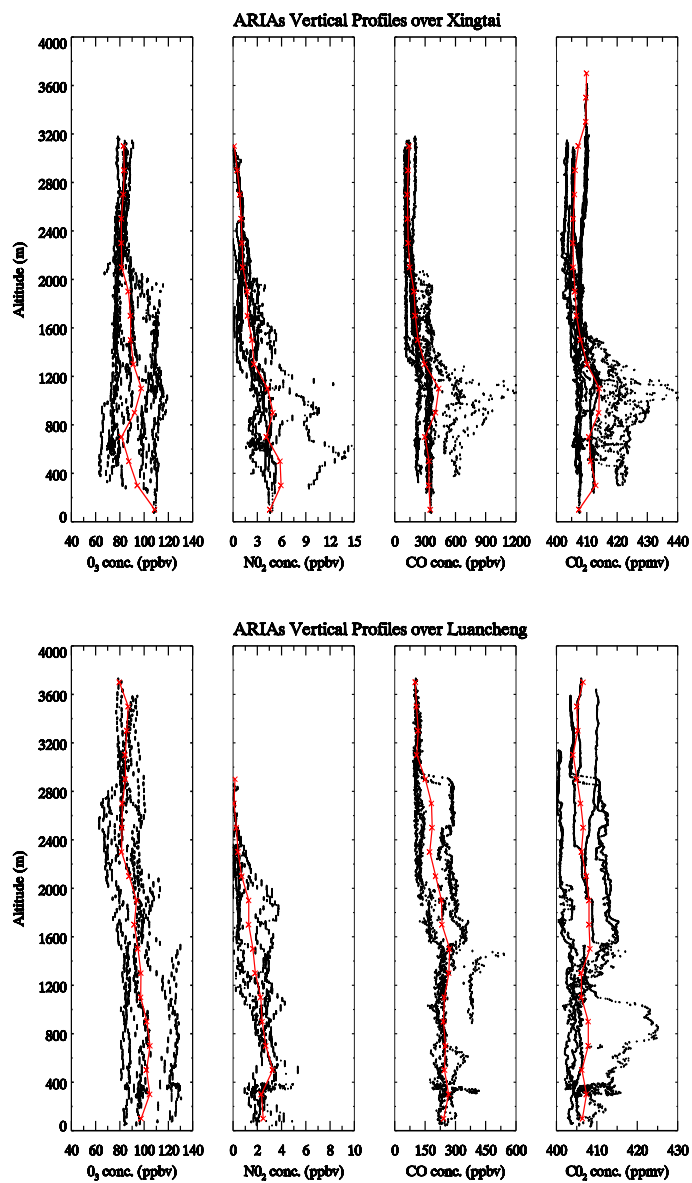
946 **Figure 2.** Summary of air pollutant concentrations in the NCP observed by Y12 aircraft. a)  $O_3$ , b)  
 947  $NO_2$ , c)  $CO$ , and d)  $CO_2$ .  
 948



949  
 950



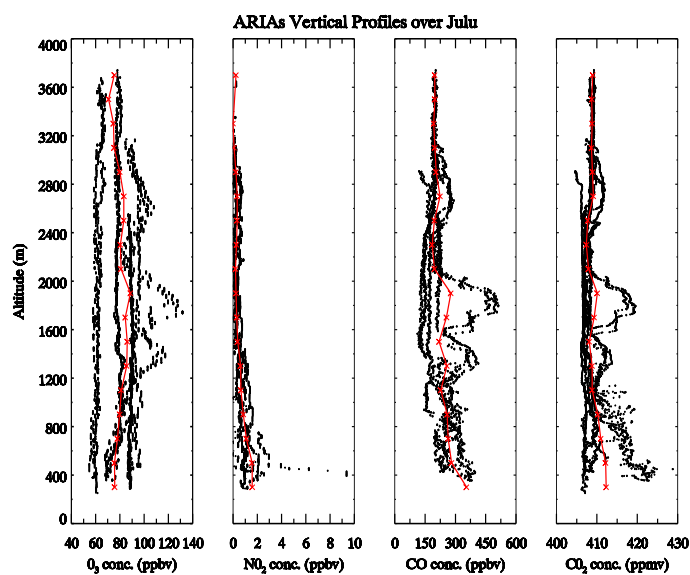
**Figure 3.** Vertical profiles of air pollutants over four locations in the NCP. a) Xingtai (XT), b) Luancheng (LC), c) Julu (JL), and d) Quzhou (QZ). Red lines show the mean profiles.



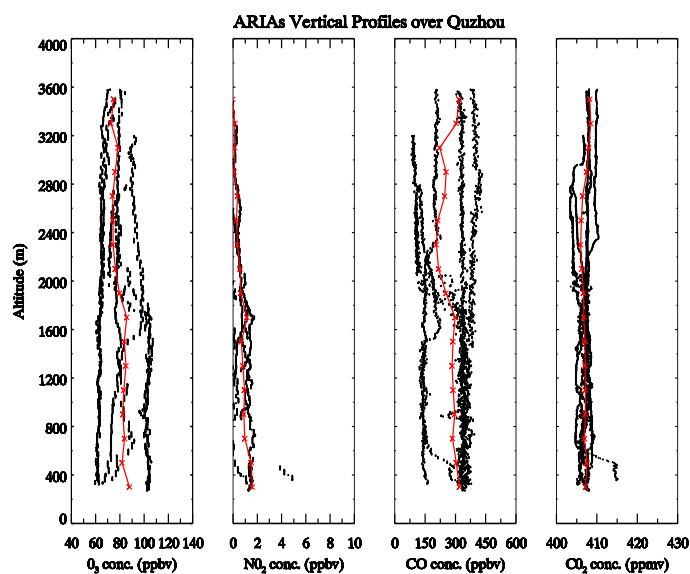




957 c)



958  
 959 d)

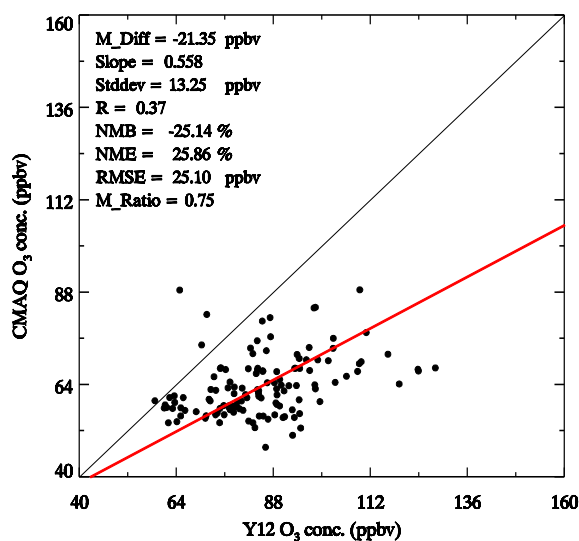


960



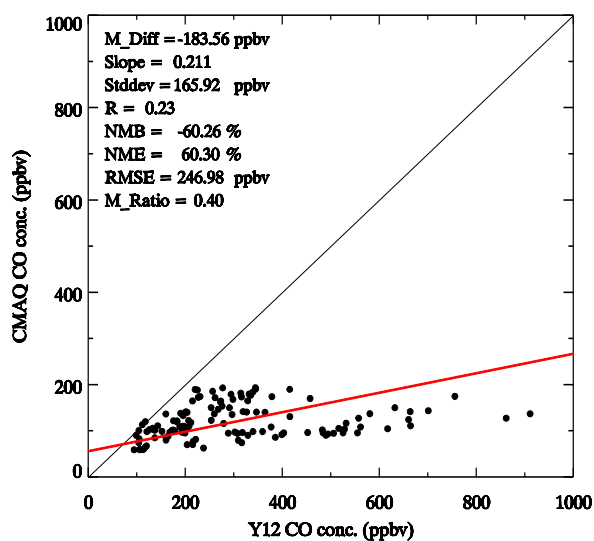
**Figure 4.** Comparison of 10-min averaged aircraft data and CMAQ simulations from 11 ARIAs research flights. a) O<sub>3</sub>, b) CO, c) NO, and d) NO<sub>2</sub>. Black line shows the 1:1 ratio; red line stands for the linear regression fitting line. M\_Diff: mean difference; R: correlation; NMB: normalized mean bias; NME: normalized mean error; RMSE: root-mean square error; M\_Ratio: mean ratio.

a)



966

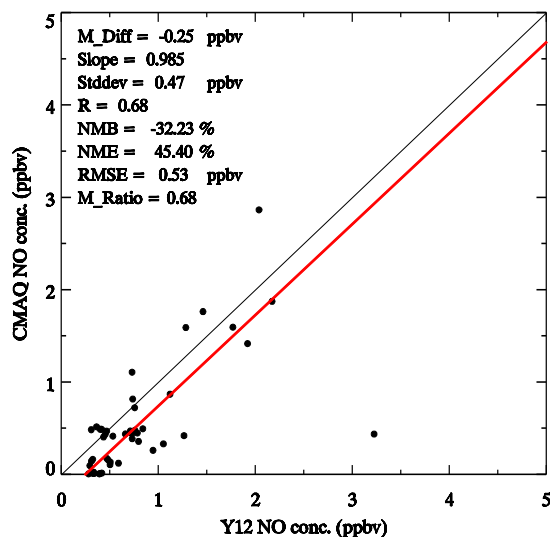
967 b)



968

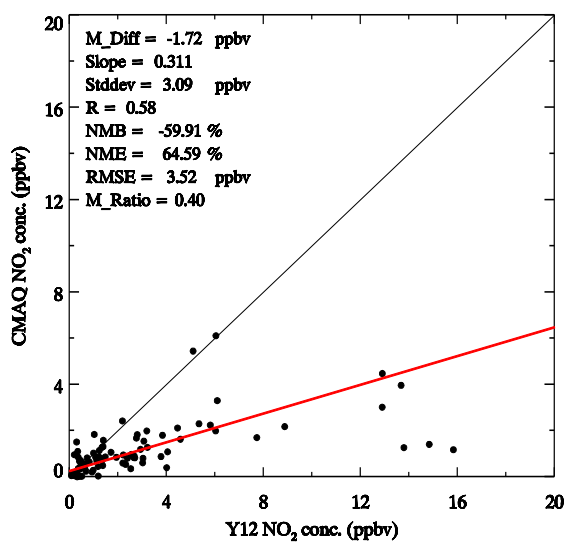


969 c)



970

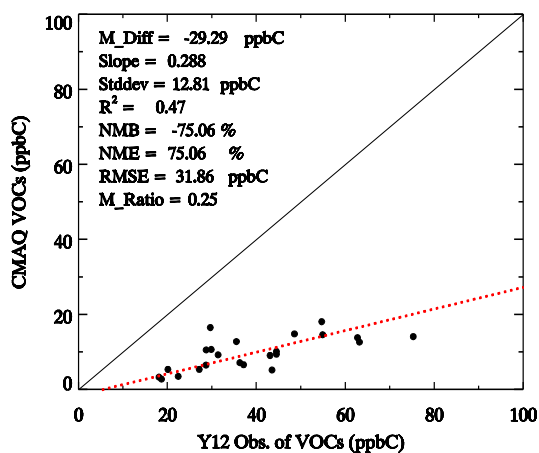
971 d)



972



**Figure 5.** Comparison of total VOCs concentrations from WAS samples and CMAQ simulations. Values are in unit of parts per billion Carbon (ppbC). Black line shows the 1:1 ratio; red line stands for the linear regression fitting line. M\_Diff: mean difference; R: correlation; NMB: normalized mean bias; NME: normalized mean error; RMSE: root-mean square error; M\_Ratio: mean ratio.

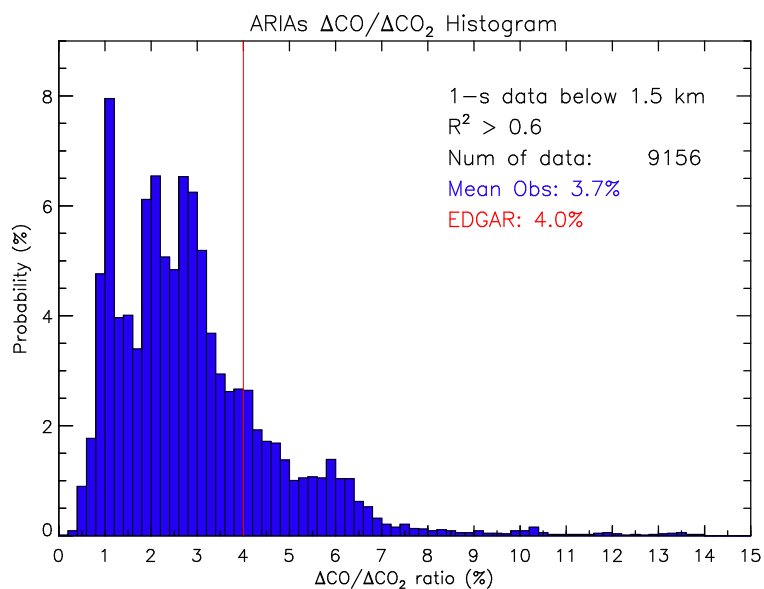


978

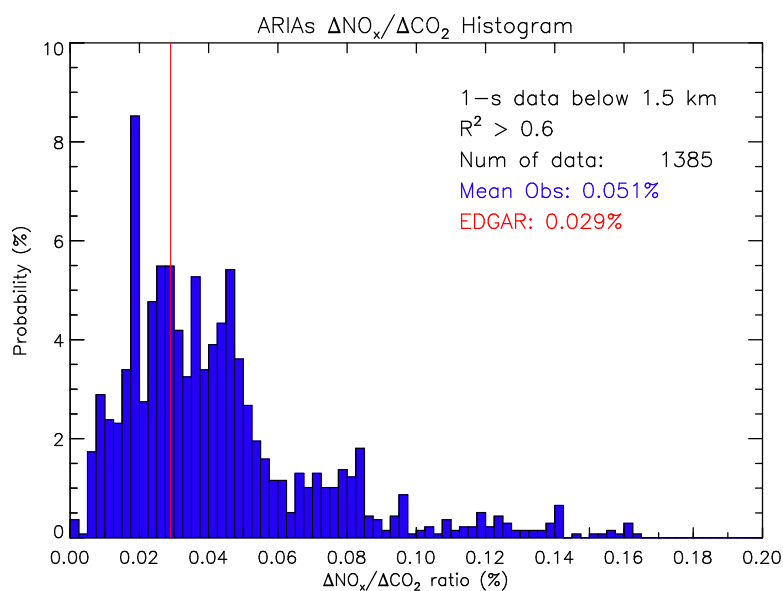


**Figure 6.** Comparison of emission enhancements (EEs) from the ARIAs campaign and emission factors (EFs) from the EDGAR emission inventory. a)  $\Delta\text{CO}/\Delta\text{CO}_2$ , b)  $\Delta\text{NO}_x/\Delta\text{CO}_2$ , c)  $\Delta\text{NO}_x/\Delta\text{CO}$ . Blue histogram shows the distribution of EEs observed by the Y12 aircraft; red line shows the ratio calculated using the EDGAR anthropogenic emissions.

a)



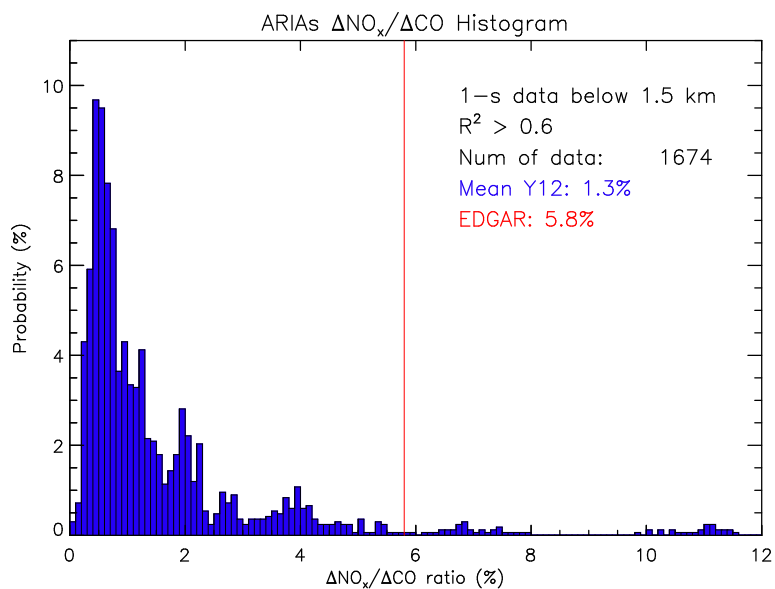
b)



986  
987



988 c)

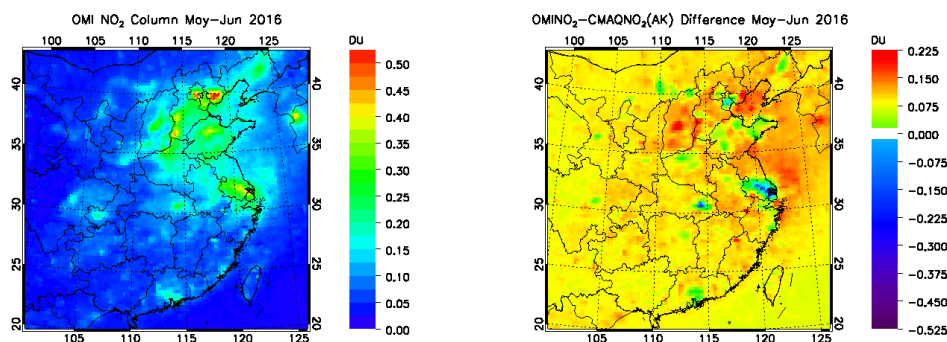


989

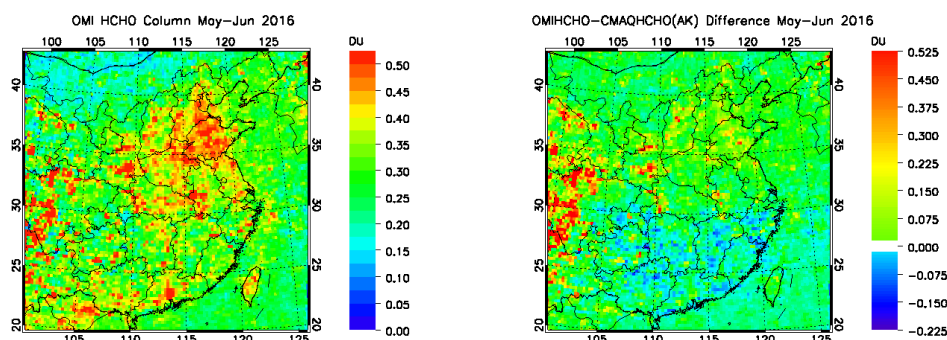


**Figure 7.** Comparison of air pollutants from satellite observations and CMAQ simulations. a) OMI NO<sub>2</sub> column (left) and the difference between OMI and CMAQ (right), Unit: Dobson Unit (1 DU =  $2.69 \times 10^{20}$  molecules/cm<sup>2</sup>); b) OMI HCHO column (left) and the difference between OMI and CMAQ (right), Unit: DU; c) MOPITT near surface CO (left) and the difference between MOPITT and CMAQ (right), Unit (ppbv).

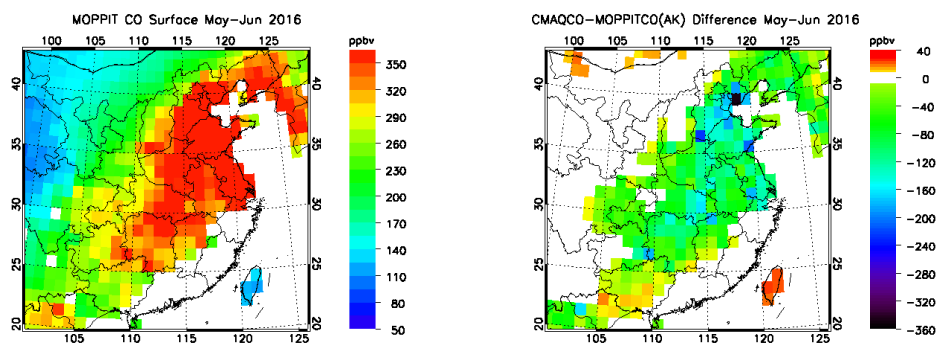
a)



b)



c)

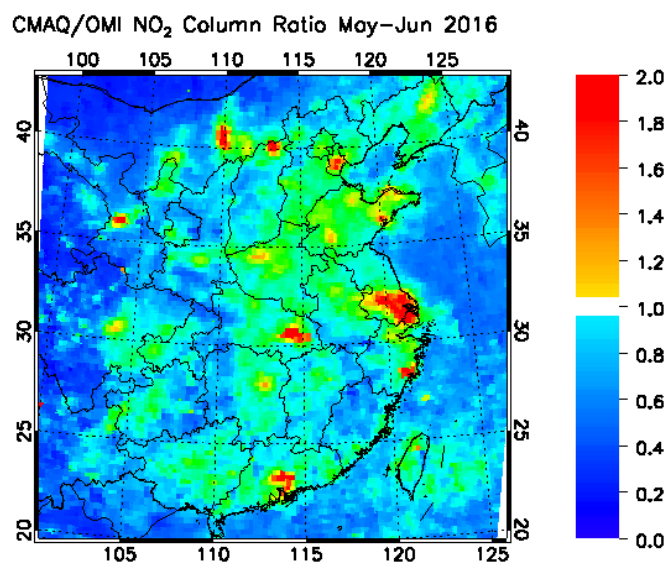
1000  
1001



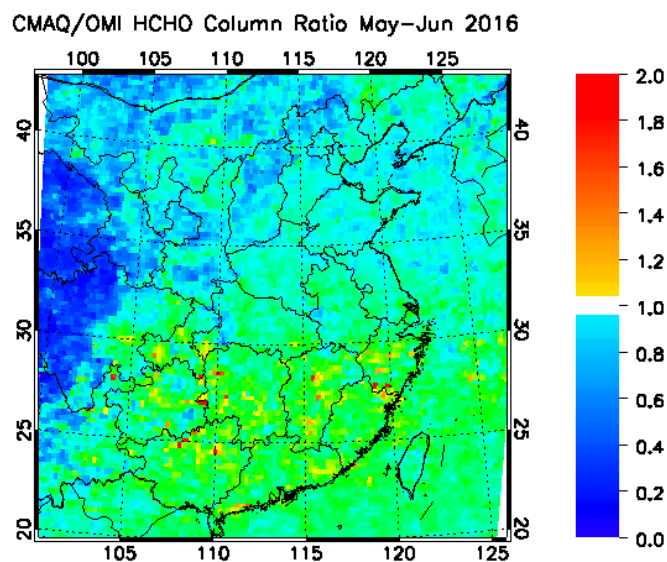


**Figure 8.** Ratios of column contents of the baseline CMAQ simulations and satellite observations. a) CMAQ/OMI NO<sub>2</sub>; b) CMAQ/OMI HCHO; c) CMAQ/MOPITT CO.

a)

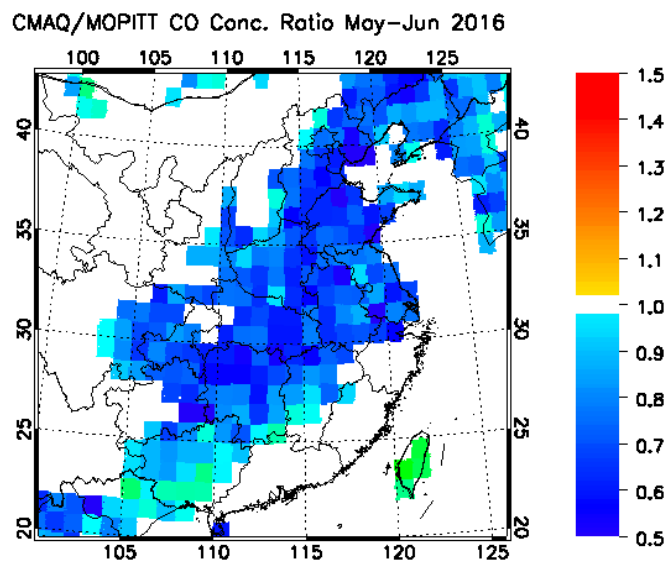


b)





1008 c)

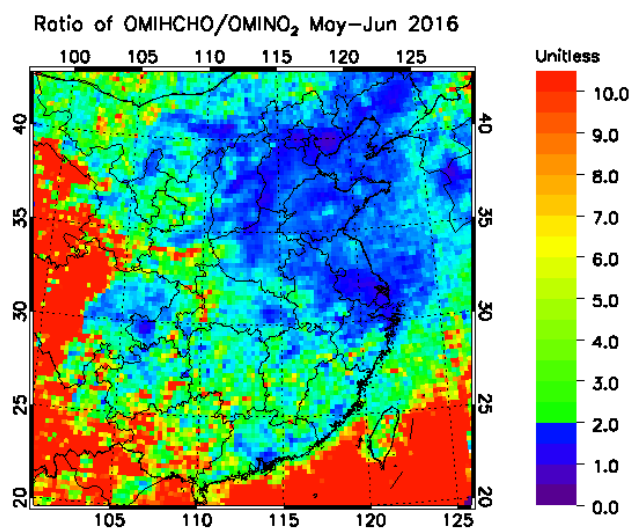


1009



**Figure 9.** Column HCHO/NO<sub>2</sub> ratios over East Asia in spring 2016. a) Ratio derived from collocated OMI HCHO and NO<sub>2</sub> observation; b) Ratio calculated from CMAQ simulations with OMI quality information and averaging kernel (AK).

a)



b)

b)

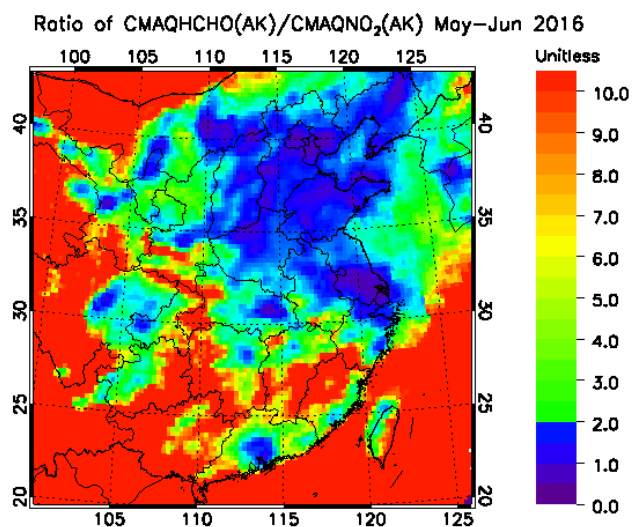
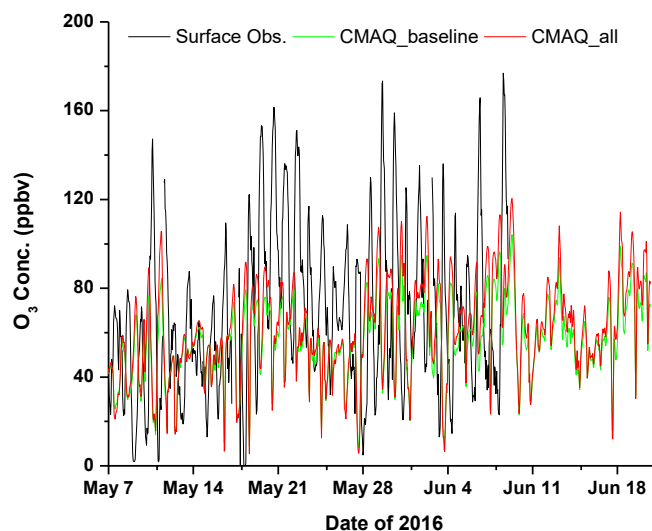
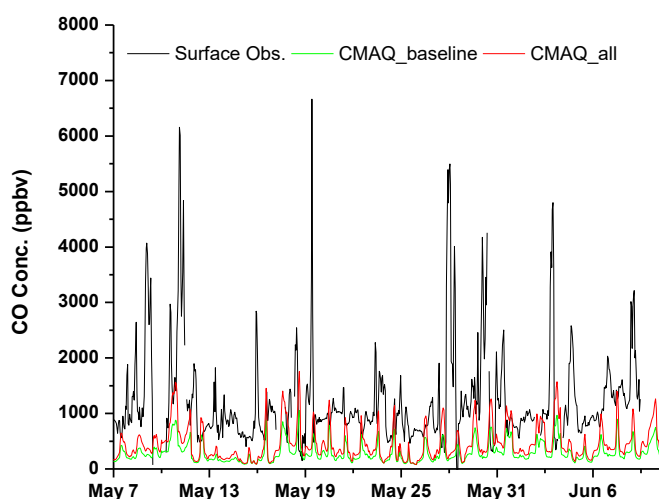




**Figure 10.** Comparison of surface hourly observations of air pollutants and CMAQ simulations at the Xingtai supersite from May to mid-June 2016. a)  $\text{O}_3$ , b) CO, c)  $\text{NO}_2^*$ , d)  $\text{NO}_x$ , and e) HCHO. \*Surface  $\text{NO}_2$  is inferred as  $\text{NO}_x - \text{NO}$  from surface observations.

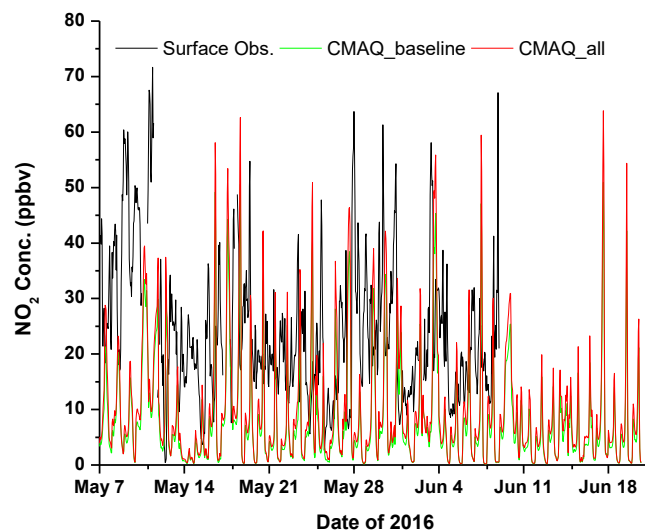


b)

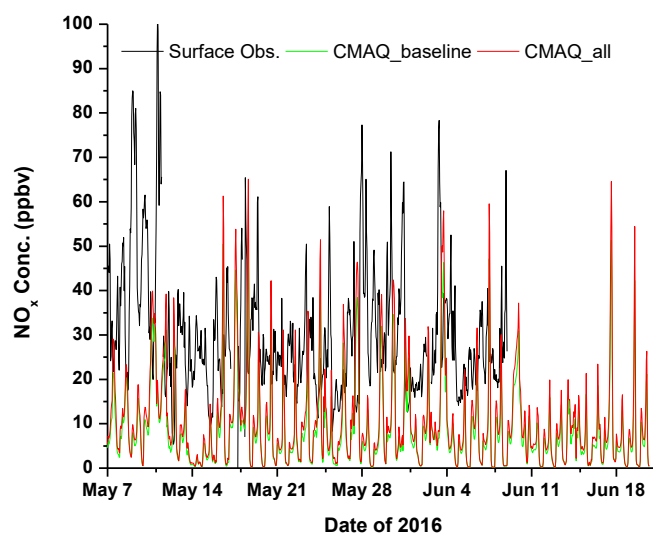




1024 c)



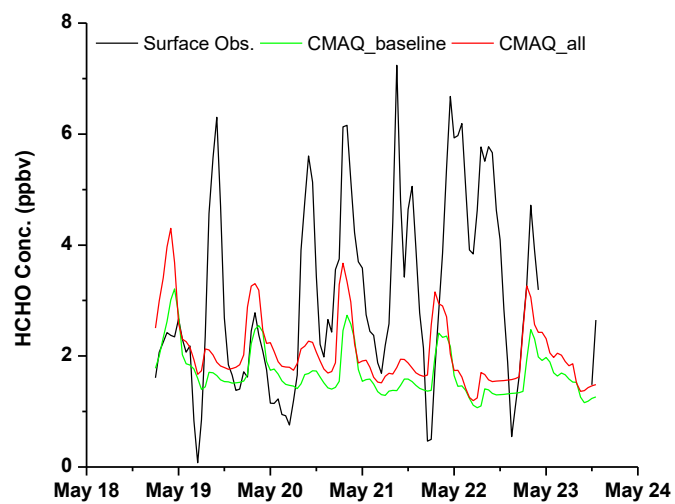
1025  
 1026 d)



1027  
 1028



1029 e)

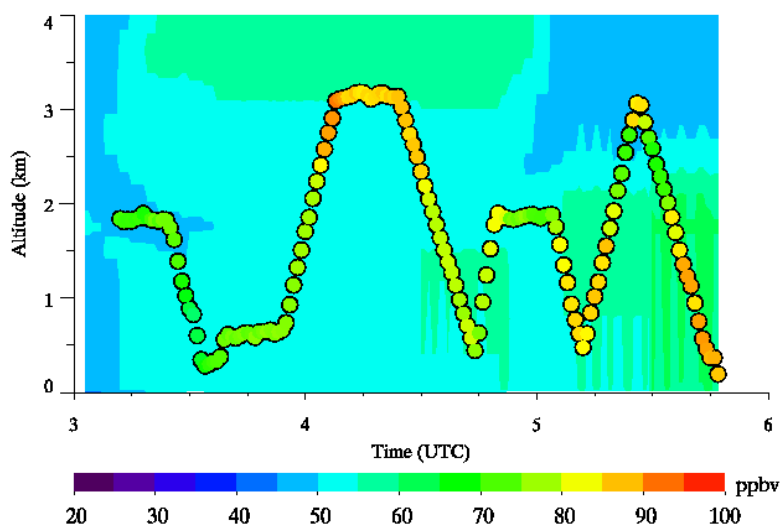


1030

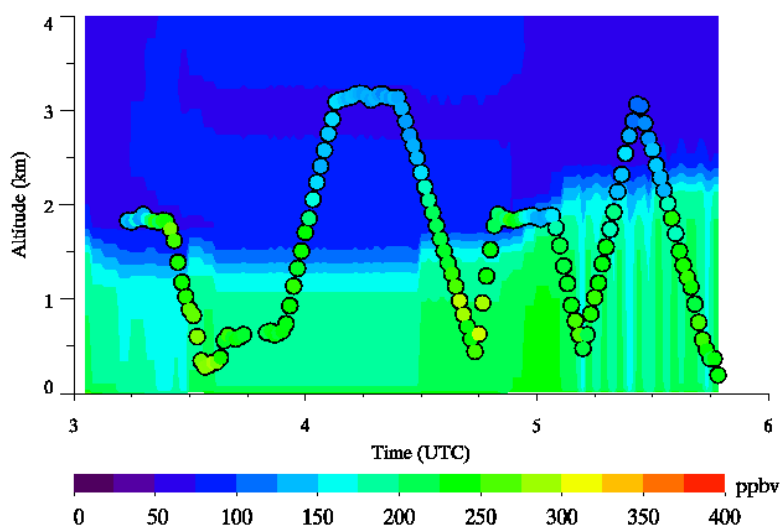




1031 **Figure 11.** A case study comparing aircraft observations and the CMAQ\_All case results on June  
1032 11, 2016. Background: CMAQ simulations. Overlay: 1 min Y12 measurements. a) O<sub>3</sub>, b) CO, c)  
1033 NO<sub>2</sub>, d) NO, and e) NO<sub>y</sub>.  
1034 a)



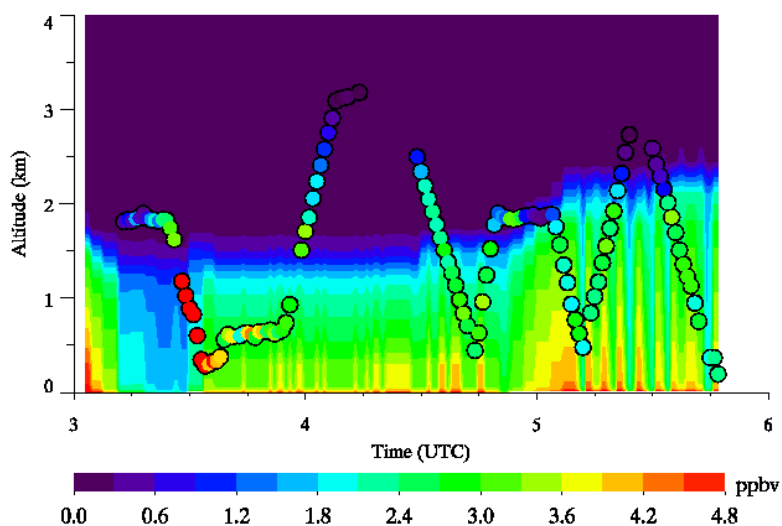
1035  
1036 b)



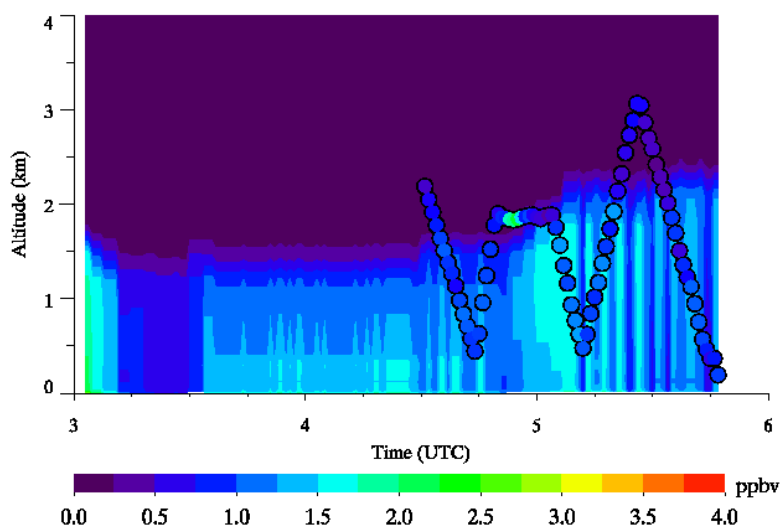
1037  
1038



1039 c)



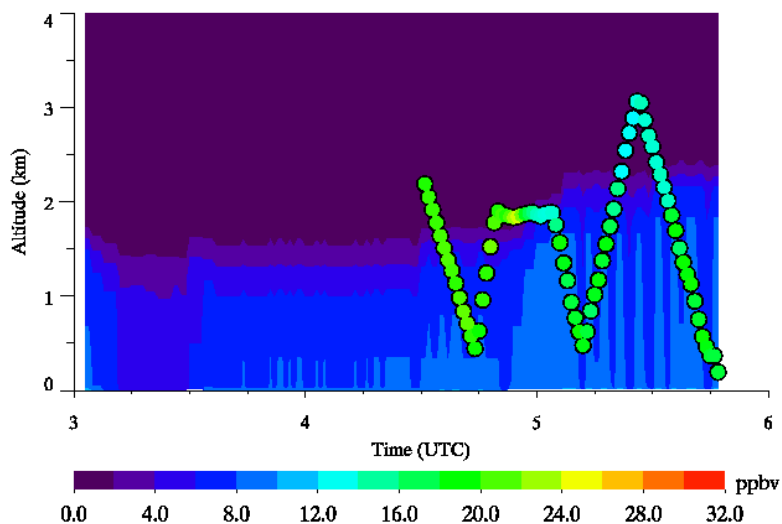
1040  
 1041  
 1042 d)



1043  
 1044



1045 e)



1046